
VAMP-NET: AN INTERPRETABLE MULTI-PATH FRAMEWORK OF GENOMIC PERMUTATION-INVARIANT SET ATTENTION AND QUALITY-AWARE 1D-CNN FOR MTB DRUG RESISTANCE

Aicha Boutorh *

National School of Artificial Intelligence (ENSIA)
Algiers, 16000, Algeria
aicha.boutorh@ensia.edu.dz

Kamar Hibatallah Baghdadi

National School of Artificial Intelligence (ENSIA)
Algiers, 16000, Algeria
kamar.baghdadi@ensia.edu.dz

Anais Daoud

National School of Artificial Intelligence (ENSIA)
Algiers, 16000, Algeria
anais.daoud@ensia.edu.dz

December 29, 2025

ABSTRACT

Genomic prediction of drug resistance in *Mycobacterium tuberculosis* remains challenging due to complex epistatic interactions and highly variable sequencing data quality. We present a novel Interpretable Variant-Aware Multi-Path Network (**VAMP-Net**) that addresses both challenges through complementary machine learning pathways. Path-1 employs a Set Attention Transformer processing permutation-invariant variant sets to capture epistatic interactions between genomic loci. Path-2 utilizes a 1D Convolutional Neural Network that analyzes Variant Call Format quality metrics to learn adaptive confidence scores. A fusion module combines both pathways for final resistance classification. We conduct comparative evaluations of unmasked versus padding-masked Set Attention Blocks, and demonstrate that our multi-path architecture achieves superior performance over baseline CNN and MLP models, with accuracy exceeding 95% and AUC of $\sim 97\%$ for rifampicin (*RIF*) and rifabutin (*RFB*) resistance prediction. The framework provides dual-layer interpretability: Attention Weight Analysis reveals Epistatic networks, and Integrated Gradients (IG) was applied for critical resistance loci (notably *rpoB*), while gradient-based feature importance from the CNN pathway uncovers drug-specific dependencies on data quality metrics. This architecture advances clinical genomics by delivering state-of-the-art predictive performance alongside auditable interpretability at two distinct levels—genetic causality of mutation sets and technical confidence of sequencing evidence—establishing a new paradigm for robust, clinically-actionable resistance prediction.

Keywords Set Attention Transformer Block (SAB) · Convolutional Neural Networks (1D-CNN) · Multi-Path Deep Learning · Interpretable Machine Learning · Genomic Variant Analysis · MTB Drug Resistance

1 Introduction

The rapid growth of high-throughput sequencing technologies has transformed genomics into a data-rich discipline, affording unprecedented opportunities to understand complex biological phenomena, such as genotype-phenotype associations and drug resistance mechanisms [Sharma et al., 2022]. Due to the contemporary requirement for personalized therapy within critical applications in *Mycobacterium tuberculosis* (MTB), drug resistance prediction from whole-genome sequencing (WGS) must be both accurate and interpretable. The prediction of drug resistance involves

*Corresponding author

a number of significant modeling challenges. First, the genetic basis of drug resistance is determined by complex, high-order epistatic interactions among variants, meaning that the models need to learn set-based relationships rather than simple sequential dependencies. Second, raw WGS data from clinical samples are inherently of varying quality, with different coverages and allele frequencies, making it crucial to robustly distinguish the true pathogenic variants from low-confidence sequencing artifacts. In other words, the model should consider the reliability (confidence) of the input data in addition to the causality (biology) thereof. Overcoming the challenges of high-dimensional, variable-length genetic variant sequences and low-quality sequencing input is crucial for developing robust and biologically valid predictive systems [James et al., 2025, Kim et al., 2022, Cosgun and Oh, 2020].

Recent advances in deep learning offer promising avenues for capturing the complex, non-local relationships inherent in genomic data [Perelygin et al., 2025]. Although CNNs have been widely applied to capture local patterns in genomic sequences, most often they require fixed-length representations and cannot model higher-order, long-range epistatic interactions among genetic variants that dictate complex phenomena such as drug resistance. This is partly overcome by Transformer-based architectures, which model non-linear, long-range dependencies using self-attention mechanisms with great success in sequence-based domains [Wu et al., 2023]; however, applications to genomic variant sequences remain sparse. Moreover, existing approaches have fallen short, either treating the genome as a dense, image-like sequence (convolutional methods) or by being heavily reliant on expert-defined features, thereby limiting the discovery of novel epistatic relationships. Crucially, most current models treat critical VCF quality metrics as binary hard filters, lacking their treatment as continuous, learnable features that could modulate the model’s confidence in a variant’s biological contribution [Eren et al., 2023].

In this work, we propose a novel Interpretable Multi-Path Fusion Architecture that strategically integrates a Set Attention Block (SAB) pathway with a dedicated, quality-aware 1D-CNN pathway to model drug resistance in MTB. We present a principled integration of a Set Transformer for learning permutation-invariant genetic causality and a 1D CNN for adaptive data quality assessment to overcome the limitations inherent in conventional sequential and feature-engineered models. The set of genomic variants (the reference-to-alternate change) is explicitly encoded with its precise position as a singular, biologically meaningful token (*ChromPosi_Ref > Alt*) processed by the SAB pathway to capture complex, high-order epistatic variant-variant interactions under the principle of permutation invariance. The 1D-CNN pathway processes multi-channel representations of critical features in VCF format, (such as *FRS* and *Genotype Confidence*), enabling the model to learn an optimal weighting of data quality rather than relying on brittle, fixed thresholds for this task. A fusion module adaptively combines the outputs of these two pathways, leveraging both global, order-agnostic biological insights and local, quality-aware representations for superior predictive performance. This integrated approach extends the Set Transformer methods to genomic variant sequences while embedding a high degree of interpretability via the attention mechanism —a crucial requirement for clinical deep learning research.

Our work introduces the novel application of the Set Transformer architecture to analyze genetic variant sequences, culminating in a robust multi-path framework that significantly outperforms traditional MLP and CNN-only baselines by treating variants as an unordered set. We adapt the SAB in a two-fold manner: first, we establish a theoretically sound baseline by applying a purely permutation-invariant model, SAB without masking [Lee et al., 2019], and second, investigate how the same architecture behaves with the incorporation of padding masks while sustaining permutation invariance. Through extensive experiments and an in-depth interpretability analysis, we show how this architectural synergy enables the Set Transformer pathway to identify and map resistance loci accurately, while the parallel 1D-CNN provides a layer of confidence. Taken altogether, our contributions uniquely marry set-based attention modeling, multimodal fusion, and interpretability, bridging a critical gap between high-performance deep learning and actionable genomic modeling for precision medicine.

The rest of the paper is organized as follows. Section 2 summarizes the related work, including some deep learning frameworks and recent progress on deep genomic learning for drug resistance. Section 3 describes the dataset of genetic variants and VCF data used in our research. Section 4 describes the proposed method and strategy in detail, including the novel interpretable two-path transformer and 1D CNN framework. The experimental results and further discussion are presented in Section 5. Finally, Section 6 summarizes our contributions and perspectives on the possible future development of this research area.

2 Related Work

Genome-Wide Association Studies (GWAS) are powerful tools for identifying genetic variants, particularly single nucleotide polymorphisms (SNPs), linked to complex traits or diseases. However, traditional GWAS methods often face limitations in handling the complexity and scale of genomic data, especially in detecting non-linear interactions and epistatic relationships between SNPs. Recent advancements in machine learning (ML) and deep learning (DL) approaches have shown great promise in overcoming these limitations, offering improved accuracy and insights in post-GWAS analysis [Sun et al., 2021, Sigala et al., 2023].

One of the primary advantages of ML over traditional statistical methods is its ability to identify complex interactions and hidden relationships between SNPs. However, traditional approaches such as linear regression (LR) are often inadequate in handling the high dimensionality and non-linearity of genomic data. Several works [An et al., 2020, Maciukiewicz et al., 2018, Zhang et al., 2012] have used penalized regression techniques, like LASSO (L1) and Ridge regression (L2), to improve model interpretation and performance by shrinking coefficients, which helps in identifying significant SNPs with greater accuracy [Sigala et al., 2023]. But as mentioned previously and due to the Curse of Dimensionality problem, the computational complexity of applying these methods to genome-wide data was inevitable, consequently leading to the development of hybrid approaches that first pre-select SNPs using statistical methods before applying ML models. Random forests (RF) and gradient boosting machines (GBM) have been widely applied in genotype–phenotype association studies due to their ability to capture non-linear relationships. For example, [Arshadi et al., 2009] showed that a GBM model was relatively robust to the inclusion of irrelevant SNPs, making it more tolerant to noise. Bayesian network methods have also been explored for modeling SNP–SNP and SNP–phenotype associations [Sigala et al., 2023, Kang et al., 2015, Ma et al., 2022]. Support Vector Machines (SVMs) and Artificial Neural Networks (ANNs) are also used; while they show promise, benchmarking suggests they do not consistently outperform other methods, and their performance depends strongly on the size and quality of input data [Nicholls et al., 2020, Sigala et al., 2023]. For example, studies on GWAS-case–control data have shown that encoding schemes (e.g., additive vs. homozygous/heterozygous) may affect classifier performance [Mittag et al., 2015]. Artificial Neural Networks have also been applied to SNP-based classification, with some studies discussing how SNP encoding (e.g., homozygous/heterozygous representation) may affect performance [Sigala et al., 2023]. Deep learning models, such as the ExPecto framework [Zhou et al., 2018] have demonstrated significant improvements in predicting the functional effects of SNPs across various tissues. ML methods are particularly effective in post-GWAS prioritization, where the goal is to narrow down the list of significant SNPs and genes identified during the GWAS stage. A variety of models, including logistic regression (LR), SVM, RF, GB, and ANN, have been applied to prioritize disease loci. [Nicholls et al., 2020] highlighted that random forests were top performers for diseases like amyotrophic lateral sclerosis and chronic kidney disease, emphasizing the importance of ensemble methods in improving prediction accuracy.

Other works adopt the approach of merging several techniques to enhance the performance of genotype–phenotype analysis and SNP prioritization. Combining machine learning models like random forests with traditional statistical methods has proven effective in improving prediction accuracy and scalability. [Silva et al., 2022] demonstrated that random forest-based dimensionality reduction techniques can efficiently shrink the dataset size while preserving key genetic information. In their approach, random forest was used to rank SNPs according to their relevance, followed by clustering of the top-ranked SNPs for more focused analysis. Other studies combined RF (for SNP selection) and used KNN and SVM algorithms to classify the identified SNPs for their association with asthma [Gaudillo et al., 2019]. Studies in [Boutorh and Guessoum, 2016, 2015, 2014] focused on dimensionality reduction in the genomic context, where their hybrid framework based on association rule mining (ARM), grammatical evolution, and neural networks addressed the “large p, small n” challenge (i.e., large features, relatively few samples) by selecting informative SNP-sets and reducing feature space prior to classification.

The application of deep learning (DL) models presents significant advancements, particularly in overcoming the limitations associated with ML methods and traditional statistical methods, such as linear models, that struggle with high-dimensional genomic data. One of the primary advantages of DL models (especially CNNs) is their capacity to model non-linear interactions between SNPs, as well as their ability to incorporate epistatic relationships, which can enhance the accuracy of disease association predictions. For instance, [Liu et al., 2018] introduced DEOPEN, an artificial neural network that combines a deep convolutional network with a three-layer feed-forward neural network to predict chromatin accessibility and evaluate genetic variants in breast cancer. Authors in [Liu et al., 2019] further developed an independent deep CNN model for predicting phenotypic traits from SNP data, employing a saliency map visualization method to identify significant biomarkers and demonstrating improved accuracy over traditional statistical methods. Similarly, [Romagnoni et al., 2019] utilized dense neural networks with various architectures, achieving

competitive mean AUC scores around 0.80 in classification tasks. [Wang et al., 2019] introduced a deep mixed model that integrates CNN and Long Short-Term Memory (LSTM) architectures. Another key example of this is the ExPecto framework developed by [Zhou et al., 2018], which utilizes deep convolutional neural networks, L2-regularized linear models, and spatial feature transformation techniques for *in silico* prediction of gene expression and disease risk. Similarly, DeepSEA [Zhou and Troyanskaya, 2015] offers a deep learning framework that uses convolutional layers to predict the effects of noncoding variants by learning regulatory sequences from chromatin-profiling data. It integrates various chromatin information to capture complex interactions, enabling precise single-nucleotide predictions and aiding in prioritizing functional variants like eQTLs and disease-associated variants. DeepWAS [Arloth et al., 2020] integrates deep learning predictions of regulatory effects into a multivariate GWAS framework, addressing the challenge of linking genetic variants to their functional roles. By annotating SNPs for regulatory potential and using regularized regression models, DeepWAS reduces the multiple testing burden and incorporates current regulatory predictions. This method has been successfully applied to GWAS data for conditions like multiple sclerosis and major depressive disorder, effectively identifying functionally relevant SNPs. Another model is DeepCombi [Mieth et al., 2021] which addresses the issue of missing heritability in traditional GWAS methods by combining convolutional neural networks (CNNs) with GWAS analyses to capture complex genetic interactions and multi-locus effects. Others like [Kwon et al., 2022] also utilized CNNs to develop CNN-GWAS that focus on enhancing the early diagnosis of atrial fibrillation (AF). Another example is the GenNet framework [van Hilten et al., 2021] designed to tackle the complexities of interpreting genetic data in GWAS while addressing computational challenges. It managed to outperform traditional methods, achieving significant accuracy and identifying both well-replicated and novel genes linked to traits such as hair color and schizophrenia.

Transformer-based architectures are also widely used with genomic data, particularly for their ability to handle large sequence data, which is often the case with long DNA sequences. One of the leading models is DNABERT, introduced in [Ji et al., 2021], a pre-trained Bidirectional Encoder consisting of 12 transformer blocks, designed to capture k-mer representations of DNA for downstream tasks such as promoter and enhancer recognition. Another work introduced LOGO [Yang et al., 2022], a lightweight language model that combines self-attention and convolutional layers to efficiently interpret non-coding regions of the human genome at high resolution, demonstrating improved performance with fewer parameters. More recent developments have extended these approaches by integrating hybrid convolution–transformer designs, hierarchical attention mechanisms, and domain-specific pretraining strategies to better capture long-range dependencies while maintaining computational efficiency.

Research in [Green et al., 2022] trained convolutional neural networks on variants from 18 genomic loci across $> 10\text{ k M. tuberculosis}$ isolates to predict resistance to 13 drugs; their multi-drug CNN (MD-CNN) and single-drug CNNs achieved high AUCs and, using saliency mapping, recovered known resistance sites while nominating novel candidate positions for further validation. [Kuang et al., 2022] compared traditional ML classifiers and CNNs on whole-genome sequence–derived features to build a fast, practical pipeline for calling TB drug resistance; they showed that carefully tuned classical models can match deep models on many tasks and presented workflows optimized for clinical turnaround. GWAS-derived SNP sets and deep learning (CNN) were used in [Kwon et al., 2022] to predict phenotype (atrial fibrillation) from genotype, demonstrating how GWAS hits can be repurposed as structured inputs for predictive models and highlighting pitfalls and opportunities of transferring association signals into individual-level predictors. A recent research work [Saliba et al., 2025] introduced group-association modeling to jointly model correlated resistance phenotypes across pathogens, leveraging shared patterns to boost sensitivity for multi-drug resistance detection while keeping model complexity low. [Deelder et al., 2019] present flexible machine-learning frameworks that take large numbers of WGS-derived predictors to classify resistant vs susceptible *M. tuberculosis* isolates; their results demonstrate robust predictive performance across drugs and emphasize scalable feature handling and interpretability for clinical usage. [Gröschel et al., 2021] deliver GenTB, a user-facing ML pipeline and web tool that integrates WGS inputs with trained models to predict TB resistance profiles; they benchmark the system against other tools, prioritize usability for labs, and provide transparent outputs to aid interpretation in clinical workflows. TB-DROP [Wang et al., 2024], an end-to-end deep learning model that consumes whole-genome mutation matrices to predict drug resistance and provide a lightweight GUI; the work focuses on clinical applicability with fast per-sample runtime and validate performance on diverse cohorts. An MDPI Diagnostics study systematically evaluates multiple ML strategies on mutation-based inputs for resistance prediction, comparing feature engineering pipelines and classifiers, and discussing limits in generalization that underscore the need for diverse training cohorts and robust external validation [Paredes-Gutierrez et al., 2025].

In summary, recent advancements in genomic data analysis reflect a clear evolution from traditional GWAS and classical machine learning methods toward more sophisticated hybrid and deep learning architectures. These modern approaches

increasingly integrate statistical modeling, feature selection, and end-to-end representation learning to capture the complex, non-linear relationships inherent in genomic data. Despite these advances, several key challenges remain unresolved—particularly those concerning model interpretability, cross-population generalizability, and the scalability of learning algorithms to high-dimensional, heterogeneous variant data. Addressing these challenges requires the development of architectures capable of unifying biological interpretability with data-driven representation power. The following sections describe the dataset and our proposed interpretable multi-path deep learning framework, designed specifically to meet these needs.

3 Data Description

Data for this study were obtained from Comprehensive Resistance Prediction for Tuberculosis: an International Consortium (CRyPTIC) [Consortium, 2022]. This globally important resource consists of a robust set of 12,289 clinical isolates of *Mycobacterium tuberculosis*, collected from 23 countries. Importantly, the dataset provides matched whole-genome sequencing (WGS) information with quantitative Minimum Inhibitory Concentration (MIC) measurements for 13 essential antitubercular drugs, covering the entire treatment landscape: first-line agents (rifampicin, isoniazid, ethambutol), key second-line drugs (amikacin, kanamycin, rifabutin, levofloxacin, moxifloxacin, ethionamide), and newer/repurposed therapeutics (bedaquiline, clofazimine, delamanid, linezolid).

The genetic data is provided in variant call format (VCF) files with variants mapped against the *M. tuberculosis* H37Rv reference genome (NC000962.3). Each VCF file contains several key features:

- GT (genotype) indicates the called allele at each position;
- DP (depth) represents total read depth at the variant site;
- COV_REF and COV_ALT provide reference and alternate allele coverage respectively;
- DPF (depth fraction) indicates the proportion of reads supporting the variant;
- GT_CONF (genotype confidence) gives the likelihood ratio for the called genotype;
- GT_CONF_PERCENTILE normalizes this confidence score; and
- FRS (a custom score) reflects variant quality.

These features allow for detailed quality assessment of variant calls and enable filtering based on sequencing depth, allele balance, and call confidence.

The phenotypic data includes both continuous MIC values and binary resistance classifications (resistant/susceptible) based on epidemiological cutoff values, with 88% of isolates having complete profiles across all 13 drugs. The dataset is enriched for drug resistance, with 55.4% of isolates resistant to at least one drug. The complete dataset is publicly available at ftp://ftp.ebi.ac.uk/pub/databases/cryptic/release_june2022/.

4 Methodology

Our approach introduces a novel Variant-Aware Multi-Path Network (*VAMP-Net*) that synergistically couples a Set Transformer architecture with a quality-aware 1D-Convolutional Neural Network for genetic variant analysis. This framework is designed as a two-branch fusion model (Figure 1).

The first branch, a Set Transformer, is specifically engineered to process the genetic variant sequence as an unordered set of tokens. This branch employs the Set Attention Block (SAB) to capture the complex non-sequential relationships between the variants, reflecting the inherent permutation-invariant nature of a set.

The second branch of our framework is a quality-aware 1D-CNN. This path focuses on local sequential features. For each variant, it takes as input a corresponding quality score sequence. The 1D-CNN is efficient in capturing the pattern in these local quality signals, thus offering the model critical information on the confidence and reliability of a variant call.

Finally, the outputs of the Set Transformer and the 1D-CNN branches are fused through a late-fusion mechanism, as presented in the Figure 1. The representations from both branches are concatenated and passed to a final classification

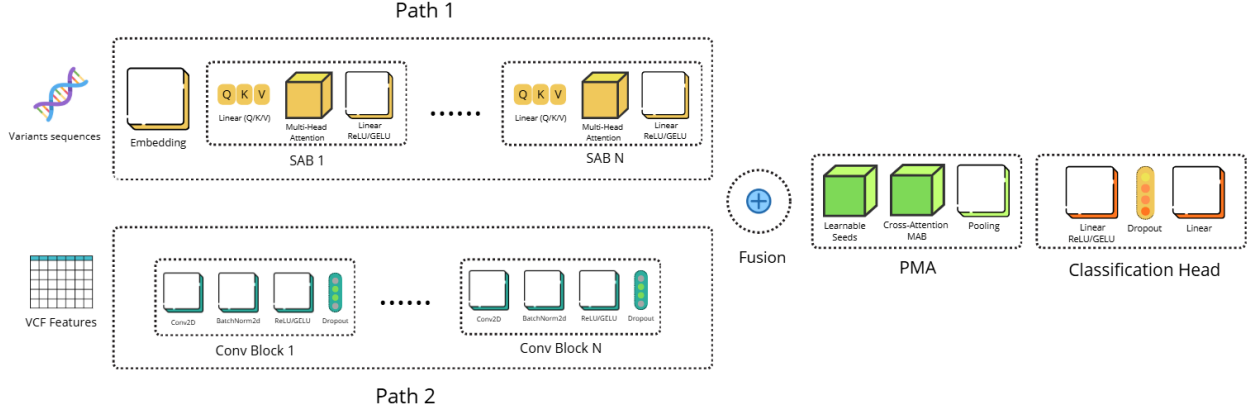


Figure 1: Overview of the Variant-Aware Multi-Path Network (VAMP-Net) Architecture

layer. This fusion allows the model to make predictions based on a rich, multi-faceted understanding of the data: the global, set-based relationships between variants from the SAB, and the local, sequential quality signals from the 1D-CNN. This multi-scale learning (local + global) provides both robustness (resistance to noisy data) and biological interpretability (attention highlighting key variants).

To formulate the problem addressed, a genomic sample is represented as a set of N genetic variants: $V = \{v_1, v_2, \dots, v_N\}$ where each variant v_i is described by $(\mathbf{g}_i, \mathbf{f}_i)$, with \mathbf{g}_i representing a sequence of genetic alteration and $\mathbf{f}_i \in \mathbb{R}^d$ denoting the associated feature vector extracted from Variant Call Format (VCF) files. The prediction task is binary classification: $y = f_\theta(V)$, where $y \in \{0, 1\}$ indicates resistance or susceptibility to a given drug, and f_θ is a parameterized deep learning model.

4.1 Data Representation: Genetic Variants as a Set of Tokens

The dataset used in this study comprises genetic variant sequences of *Mycobacterium tuberculosis* (MTB), as described in Section 3. Each sample is represented by a set of all identified genetic variants, resulting in sequences of variable length.

Transformer-based architectures have fundamentally transformed the processing of sequential data, exhibiting remarkable ability to capture long-range dependencies and contextual relationships. In the genomics domain, recent transformer models have achieved promising results; however, most existing approaches primarily rely on reference DNA sequences or *K-mer* tokenization as inputs [Consens et al., 2025]. While such representations effectively capture local sequence patterns, they often treat variants as abstract tokens embedded within a continuous sequence. This abstraction can obscure the explicit biological relationships and combinatorial interactions among individual genetic alterations—relationships that are essential for understanding complex traits such as drug resistance.

To address this limitation, we propose a variant-centric representation that explicitly encodes both the molecular identity and genomic position of each variant as a single, biologically meaningful token. In this framework, each token directly represents a specific reference-to-alternate allele substitution, enabling the model to learn variant-level interactions rather than merely sequence-level dependencies. This transition from sequence-level attention to variant-level interaction attention provides a more interpretable and biologically grounded foundation for modeling genotype–phenotype associations. Specifically, we employ an attention mechanism that operates on a *ChromPos_Ref > Alt* representation, designed to capture biologically meaningful variant–variant interactions. In this representation, each genetic variant \mathbf{a}_k is uniquely identified by its chromosome, precise genomic position, reference allele, and alternate allele (e.g., *chr1:12345:A>G*). This compact and canonical identifier serves as a semantically rich token, allowing each sample’s genomic profile \mathbf{g}_i to be expressed as a discrete set of variant tokens T : $\mathbf{g}_i = \{a_1, a_2, \dots, a_T\}$. Such a representation enables the transformer to reason directly over meaningful biological entities—facilitating the discovery of high-order, non-linear relationships among variants that underlie phenotypic

outcomes such as drug resistance.

This representation is particularly well-suited for a permutation-invariant modeling framework. By adopting this symbolic encoding, the entire collection of genetic variants for each sample can be treated as a set rather than an ordered sequence. This design allows the model to learn complex, non-linear dependencies and interactions among variants independent of their order in the dataset or genome file. The proposed tokenization strategy therefore serves as a key enabler of our set-based learning paradigm, marking a distinct shift from conventional sequence-oriented approaches and focus on the intrinsic relationships between variants themselves.

4.2 Model Architecture: Variant-Aware Multi-Path Network (VAMP-Net)

Variant-Aware Multi-Path Network (*VAMP-Net*), a dual-path deep learning framework specifically designed to address the limitations of conventional single-stream models in genomic data analysis. *VAMP-Net* is architected to process two distinct sources of information essential for robust variant-based prediction (Figure 1): (1) the symbolic identity and biological context of each genetic variant and (2) the quality metrics of quantitative sequencing that reflect data reliability.

The rationale for this dual-path design is twofold: first, to leverage the inherent set-based nature of a sample’s variant, where order is non-critical, by using a modern attention mechanism; and second, to capture local patterns and dependencies within the associated quality signals using convolutional processing.

The framework is structured as follows:

- Path-1 – Symbolic and Topological Stream: Processes the set of genomic variants using a symbolic tokenization scheme at variant-level, allowing the model to learn relationships regardless of input order.
- Path-2 – Feature and Sequential Stream: Processes a structured sequence of quantitative and contextual features (e.g., read depth, genotype quality) using one-dimensional convolutional layers to extract local quality patterns.

The outputs from both pathways are subsequently fused to form an integrated latent representation, which is passed to a final prediction head. This fusion allows *VAMP-Net* to jointly reason over global, biologically meaningful variant interactions and local, quality-aware signals, thereby offering a comprehensive and interpretable foundation for genomic variant modeling.

4.2.1 Path-1: Set Attention Transformer Block (SAB) on Genetic Variants

We address the modeling of genetic variant sequences for downstream tasks of drug resistance prediction. Each sample \mathcal{X}_i consists of a variable-sized set $\mathcal{X}_i = \{x_1, x_2, \dots, x_T\}$ where each element x_k represent a specific genetic variant. Since \mathcal{X}_i is an unordered set, the architecture must satisfy **permutation invariance**, formulated in Equation 1:

$$f(\pi \mathcal{X}_i) = f(\mathcal{X}_i), \quad \forall \pi \in S_n, \quad (1)$$

where π denotes a permutation operator on the sequence elements. The first branch of our model is a Set Transformer, a deep learning architecture specifically designed to operate on sets presented in Figure 2. Its core component, the Set Attention Block (SAB), replaces the standard transformer’s multi-head attention mechanism. Unlike standard transformers which rely on positional encodings and often causal masks for sequential data, the SAB is inherently permutation-invariant. This means the model’s output is independent of the order of the input tokens. For our genetic variant sequences, where the order is arbitrary, the attention mechanism’s ability to model interactions among all elements in a set without relying on their positions is a critical advantage. This enables the model to learn a unified representation of the set, a property that is essential for our application.

The SAB pathway models variant-variant interactions while maintaining permutation invariance. For an input sequence represented by a matrix $\mathbf{X} \in \mathbb{R}^{n \times d_{model}}$, where n is the sequence length and d_{model} is the embedding dimension, the SAB computes attention scores between all pairs of tokens in the input sequence, followed by a weighted sum of the values. Mathematically (Equation 2), for an input set of tokens:

$$\text{Attention}(\mathbf{Q}, \mathbf{K}, \mathbf{V}) = \text{softmax} \left(\frac{\mathbf{Q}\mathbf{K}^\top}{\sqrt{d_k}} \right) \mathbf{V} \quad (2)$$

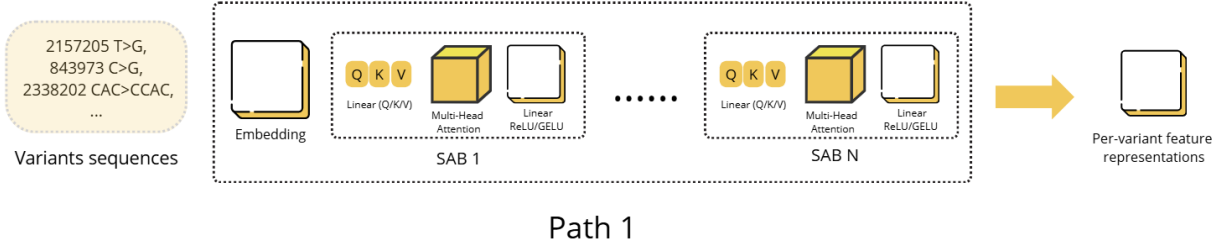


Figure 2: Path-1 Architecture: Set Attention Transformer Block (SAB) for Symbolic Variant Processing

where d_k is the dimension of the keys. Unlike standard transformers, **no causal mask** is applied to preserve permutation invariance. The output of SAB is aggregated using a pooling operator ρ as formulated in Equation 3:

$$\mathbf{z}_{\text{SAB}} = \rho(\text{SAB}(\mathbf{X})) \quad (3)$$

We apply the Set Attention Block (SAB) in two distinct configurations, which were investigated to assess the impact of explicit padding utilization:

I - Unmasked Set Attention:

The first contribution adapts the Set Transformer framework [Lee et al., 2019] of the unmasked SAB for modeling genetic variant sequences represented as unordered tokens. Unlike standard transformers for sequential data, no attention masks —neither causal masks is applied, ensuring each variant can attend to every other variant without positional or causal constraints, nor padding masks is applied. This model serves as a theoretically pure baseline for evaluating the efficacy of a purely permutation-invariant approach. The input to the model is a batch of padded sequences, where each variant is represented by its token embedding. Within the SAB, the self-attention mechanism computes attention scores for every token pair, including those involving the meaningless padding tokens. The model learns to encode the relationships between all tokens, with no explicit instruction to ignore the padded ones. This approach tests the model’s capacity to learn a meaningful representation of the data despite the presence of noisy, non-informative tokens. The training objective is to perform a specific task of Drug Resistance, based on their set of variants. The hyperparameters for this model, including the number of SAB layers, hidden dimensions, and learning rate, are provided in the Experimental Section 5.4 .

II- Padding-Masked Set Attention :

The second contribution is the introduction of a padding mask to the attention mechanism, a crucial modification that enables efficient batching and improves computational performance. The padding mask is a binary matrix that masks out attention to the padded tokens. It is applied by adding a large negative value to the attention scores of padded tokens prior to the softmax operation.

To handle sequences of varying lengths, we introduce in Equation 4 a **padding mask** $\mathbf{M} \in \{0, -\infty\}^{N \times N}$, where:

$$M_{ij} = \begin{cases} 0, & \text{if both } i, j \text{ are valid variants,} \\ -\infty, & \text{if } j \text{ is padding.} \end{cases} \quad (4)$$

The attention computation becomes as defined in Equation 5:

$$\text{softmax} \left(\frac{\mathbf{Q}\mathbf{K}^\top + \mathbf{M}}{\sqrt{d_k}} \right) \mathbf{V} \quad (5)$$

which masks out contributions from padded positions but preserves invariance over valid variants. Since M only removes invalid tokens (not reordering them), the equivariance property still holds over the subset of valid elements (Equation 6):

$$\text{SAB}_{\text{masked}}(\mathbf{P}\mathbf{X}) = \mathbf{P}\text{SAB}_{\text{masked}}(\mathbf{X}), \quad (6)$$

\mathbf{P} a permutation matrix that reorders the tokens in \mathbf{X} . Provided M is permuted identically as formulated in Equation 7. \mathbf{M}' represents the permuted version of the padding mask \mathbf{M} that must be used when the input tokens \mathbf{X} are permuted by the matrix \mathbf{P} :

$$M' = \mathbf{P}M\mathbf{P}^\top. \quad (7)$$

The application of the padding mask \mathbf{M} provides crucial theoretical and practical advantages for processing variable-length variant sets:

- **Elimination of Irrelevant Signal:** It ensures irrelevant (padded) tokens do not contribute to attention score computation, thereby preventing the model from dedicating capacity to learning representations for non-existent variants.
- **Mitigation of Attention Dilution:** By zeroing out the influence of padding, the mask prevents artificial self-attention dilution within smaller variant sets. This maintains the true relative importance of valid tokens, particularly when a large portion of the input is padding.
- **Preservation of Set Invariance:** Since the mask is content-based (identifying the padding symbol) and not positionally fixed, it does not interfere with the core permutation invariance of the Set Attention Block, provided the mask is permuted identically with the input tokens.

4.2.2 Path-2 : Quality-Aware 1D-CNN

A second branch of our model consists of a 1D-CNN that processes the quality scores associated with each variant (Figure 3). These scores, which are typically sequential and local, provide crucial information on the confidence of each variant call. A 1D-CNN is an ideal choice for this task, as it excels at capturing local patterns, such as the relationship between a variant’s read depth (DP) and its genotype confidence (GT CONF). The 1D-CNN branch processes the variant feature matrix $\mathbf{F} \in \mathbb{R}^{N \times d}$.

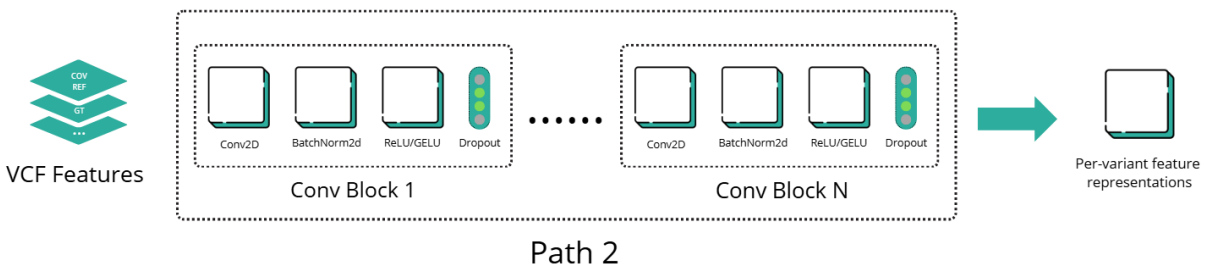


Figure 3: Path-2 Architecture: Quality-Aware 1D Convolutional Neural Network (1D-CNN) for VCF Feature Processing

While the core genetic information (CHROM, POS, REF, ALT) is fundamental, the true richness of VCF files for deep learning lies within their FORMAT fields. These fields provide critical quantitative and qualitative information about the confidence and context of each variant call, moving beyond a simple binary presence or absence of a mutation. This depth of information, often underutilized in conventional genomic deep learning approaches, represents a powerful, biologically relevant multi-channel input for sophisticated models. Using these detailed metrics, a deep learning model can gain a more nuanced understanding of the reliability and characteristics of each detected variant, which is paramount for accurate genotype-phenotype association studies, especially when dealing with potentially noisy or

low-coverage sequencing data from real-world clinical samples.

The proposed framework specifically harnesses seven VCF FORMAT fields as distinct input channels for the Convolutional Neural Network (1D-CNN). When extended to multi-channel inputs, a 1D-CNN can simultaneously process multiple features per genomic position, with each VCF field representing a distinct channel. This allows CNN to learn intricate local patterns and dependencies across these different quality and genotype metrics for each variant, rather than relying solely on the raw genotype information.

4.2.3 Multi-Path Fusion Mechanism

The final stage of the *VAMP-Net* architecture involves the integration of the learned representations from the two specialized paths. The outputs of the two branches—the SAB’s permutation-invariant set representation (\mathbf{z}_{SAB}) from Path-1, and the 1D-CNN’s quality-aware feature vector (\mathbf{z}_{CNN}) from Path-2—are concatenated to form a comprehensive, fused representation $\mathbf{z}_{\text{fused}}$ (Equation 8):

$$\mathbf{z}_{\text{fused}} = [\mathbf{z}_{\text{SAB}}; \mathbf{z}_{\text{CNN}}] \quad (8)$$

This late-fusion approach is crucial, as it allows each branch to specialize independently in its unique data modality (symbolic variant topology vs. quantitative feature sequence) before their insights are combined. The fused vector is then passed through a fully connected network to a final output layer for the prediction of drug resistance.

To determine the optimal strategy for combining these disparate signals, we investigate three distinct modulation mechanisms between the output of Path-1 (transformer) and Path-2 (1D-CNN):

1. Suppression (De-emphasis of Quality):

The first fusion mechanism is inspired by LSTM’s forget gate control. The purpose of this gate in LSTM is to control how much of the old state is remembered in the new state. By taking the sigmoid of the current input C_t and the hidden state H_{t-1} , values are transformed into the probability domain, and then multiplied element-wise with C_{t-1} , the past internal state.

We modify the purpose and formula of this gate to suit our case: by taking the sigmoid of Path-2, we use the additional features to control the confidence of the current variants, and then multiply the result by the output of Path-1. The Suppression fusion is defined in Equation 9, where \odot denotes element-wise multiplication.

$$\begin{aligned} \mathbf{g} &= \sigma(\mathbf{z}_{\text{CNN}}) \\ \mathbf{z}_{\text{fused}} &= \mathbf{g} \odot \mathbf{z}_{\text{SAB}} \end{aligned} \quad (9)$$

This formulation applies a multiplicative suppression to the output of Path-1 (\mathbf{z}_{SAB}). Since the modulation score \mathbf{g} is constrained to $[0, 1]$, the resulting fused vector $\mathbf{z}_{\text{fused}}$ will have element values ranging between 0 and the corresponding values in \mathbf{z}_{SAB} . In effect, Path-2’s quality features provide a scalar factor that selectively scales the influence of each variant, and if the quality metrics indicate low confidence, the variant’s representation can be driven toward 0, effectively performing a dynamic, data-driven form of variant feature selection during the fusion process.

2. Amplification (Emphasis on Quality):

The second investigated fusion strategy, *Amplification*, is designed to explicitly test the hypothesis that quality and low-level features (Path-2) provide a critical signal gain to the core symbolic variant representation (Path-1). This mechanism ensures that high-quality, high-confidence variants can have proportionally increase in impact, thereby emphasizing a robust subset of the data.

Unlike the Suppression mechanism, this formulation guarantees that the symbolic representation \mathbf{z}_{SAB} is always passed through to the final output, regardless of the quality metrics. The Quality-Aware vector \mathbf{z}_{CNN} acts as an additive gain control. We adapt the gating mechanism as defined in Equation 10, where \odot denotes element-wise multiplication.

$$\begin{aligned} \mathbf{g} &= \sigma(\mathbf{z}_{\text{CNN}}) \\ \mathbf{z}_{\text{fused}} &= (1 + \mathbf{g}) \odot \mathbf{z}_{\text{SAB}} \end{aligned} \quad (10)$$

This formulation achieves a soft integration that preserves the full contribution of the core variant signal. By introducing the constant 1 into the scalar factor $(1 + \mathbf{g})$, the mechanism guarantees a baseline preservation, ensuring that the fused output $\mathbf{z}_{\text{fused}}$ is never less than the original symbolic representation \mathbf{z}_{SAB} . As the modulation score \mathbf{g} is constrained to the range $[0, 1]$, the total scalar factor $(1 + \mathbf{g})$ remains bounded within the interval $[1, 2]$. This results in a controlled form of additive gain, where the most robustly supported variants—those with high-quality metrics—receive a maximum scaling of 200% of their original magnitude. This approach avoids the risk of zeroing out potentially relevant variants, allowing all identified mutations to participate in the final prediction while prioritizing those with the highest associated confidence.

3. Adaptive Amplification & Suppression

The final fusion strategy is *Adaptive Amplification & Suppression*, designed to provide the model with a dynamic, context-aware control over the Path-1 signal. This mechanism combines the feature selection capability of *Suppression* with the signal enhancement capability of *Amplification*, allowing the influence of the symbolic variant representation (\mathbf{z}_{SAB}) to be either scaled down or scaled up based on the quality metrics (\mathbf{z}_{CNN}).

We synthesize the previous two modulation strategies by modifying the gating factor. Using the same modulation score $\mathbf{g} = \sigma(\mathbf{z}_{\text{CNN}})$, the fused vector is calculated as Equation 11.

$$\mathbf{z}_{\text{fused}} = (2 \odot \mathbf{g} - 1) \odot \mathbf{z}_{\text{SAB}} \quad (11)$$

where \odot denotes element-wise multiplication.

This adaptive mechanism creates a bipolar scaling factor which introduces a powerful, new operational dynamic. As the modulation score \mathbf{g} , derived from the quality features, is constrained to the range $[0, 1]$, the resulting scaling factor $(2 \odot \mathbf{g} - 1)$ is dynamically mapped to the closed interval $[-1, 1]$. This allows the model to continuously transition between Suppression Zone (noise filtering) and Amplification Zone (signal gain) based on the input quality. Specifically, when quality features are poor ($\mathbf{g} \approx 0$), the scaling factor approaches -1 , resulting in a negative scaling of the variant representation, effectively acting as an aggressive noise filter by reversing the polarity of low-confidence signal. Conversely, when quality features are excellent ($\mathbf{g} \approx 1$), the factor approaches 1 , leading to maximum positive scaling and thus prioritizing the most robustly supported variants. This ability to span both positive and negative scalar values allows the model to not only ignore noise but to actively penalize uncertain variants, providing a comprehensive, context-aware control signal to the final prediction layers.

4.3 Interpretability

Following the development of the Variant-Aware Multi-Path Network (*VAMP-Net*), we conducted a critical interpretability analysis to identify genomic variants and sequencing features most significantly associated with *RIF* and *RFB* resistance in *Mycobacterium tuberculosis*. Our approach is uniquely tailored to the dual-pathway model architecture, employing methods that respect the inherent structure of each stream.

4.3.1 Dual-Path Interpretability Framework

We analyzed both pathways of the *VAMP-Net* architecture separately to isolate the contribution of symbolic variant identity from that of quantitative quality metrics:

Path-1 (Set Transformer Analysis): For the SAB pathway, which processes the symbolically tokenized and permutation-invariant set of variants (\mathbf{z}_{SAB}), we applied Integrated Gradients (*IG*). This method calculated attribution scores by integrating gradients from baseline input to actual variant embeddings, measuring how each genetic variant contributed to the final resistance prediction irrespective of its ordering in the input set.

Path-2 (CNN Analysis): For the convolutional pathway processing the ordered VCF feature vector (\mathbf{z}_{CNN}), we employed gradient-based saliency analysis in conjunction with systematic feature ablation. The gradient analysis

quantified the relative importance of feature channels (e.g., DP, GT, FRS) across the sequential input. Subsequently, systematic feature ablation confirmed the findings by quantifying the drop in predictive performance when specific VCF quality metrics were masked or perturbed. This framework reliably quantifies both the positional importance of variants along the input sequence and the absolute contribution of specific VCF quality metrics.

4.3.2 Variant Importance Quantification

For Path-1, which utilizes the Set Attention Transformer, we quantified the contribution of each individual variant by applying Integrated Gradients (IG) with respect to the final classification layer output. We first extracted the variant-level embeddings from the trained symbolic tokenizer. The attribution scores were then calculated by integrating the gradients along a linear path over $N = 20$ integration steps, ensuring robust and stable gradient estimates. Finally, the calculated attribution scores were aggregated across all instances in the test cohort to obtain the mean importance measure for each unique ChromPos_Ref>Alt variant. This yields an interpretable ranking of variants based on their model-predicted association with drug resistance.

4.3.3 Feature Ablation Studies

To robustly quantify the influence of sequencing quality and context features (processed by Path-2), we conducted systematic feature ablation on individual VCF channels. This approach, designed to isolate the causal contribution of each metric, involved methodically setting the values of a single VCF feature channel to a neutral baseline (zero) across all test samples. We then rigorously measured the resulting change in the model's prediction confidence and overall performance (e.g., AUC or F_1 score).

This systematic process allowed us to identify which VCF quality metrics were most critical for accurate resistance classification and, conversely, which features introduced minimal signal. The ablation analysis specifically covered the following eight VCF feature channels, reflecting key data quality and genotype metrics: Genotype Calls (GT), Read Depth (DP), Depth Fraction (DPF), Reference Coverage (COV_REF), Alternative Coverage, (COV_ALT), Fraction of Supporting Reads (FRS), Genotype Confidence (GT_CONF), Confidence Percentiles (GT_CONF_PERCENTILE).

The resulting performance decrement for each ablated feature serves as its direct measure of importance within the VAMP-Net architecture.

4.3.4 Attention-Based Variant Interaction Analysis

To move beyond individual variant importance and uncover complex epistatic relationships between resistance-associated variants, we leveraged the intrinsic relational mechanism of the Set Attention Block (SAB) layer from Path-1. The SAB's self-attention matrix inherently encodes the model's learned pairwise dependency structure between every variant in the input set.

For each test sample, we systematically extracted the attention weights from the first SAB layer and averaged them across all attention heads to compute the raw variant relationships. The interaction strength between any two variants was thus quantified as the bidirectional attention weight between their respective tokens, which was then aggregated across the entire test cohort for statistical reliability.

This aggregated matrix was subsequently used to construct a variant interaction network. Network construction was restricted to variants exhibiting sufficient frequency and strong, recurring interaction occurrences to ensure statistical reliability. Finally, we applied modularity optimization algorithms to the network to perform community detection, thereby identifying functional modules (groups of variants) that likely operate synergistically to confer drug resistance. The highly connected nodes identified in this process were designated as hub variants, representing key drivers of the overall epistatic effect.

5 Experimentation and Discussion

This section presents the empirical validation of the Variant-Aware Multi-Path Network (**VAMP-Net**) and its core components, followed by a detailed discussion of the biological insights derived from our interpretability framework. We first detail the preparation of the dataset and the specific encoding utilized for the ChromPos_Ref>Alt variant tokens. Subsequent subsections systematically evaluate three critical aspects of the design of **VAMP-Net**: the selection of the

optimal fusion mechanism, a comprehensive performance comparison, and a deep-dive interpretation of the predictions of the final model, including variant importance and epistatic interaction networks. The goal of this analysis is not only to demonstrate superior classification performance but to validate the translational utility of our dual-path approach for genetic resistance prediction.

5.1 Data Preprocessing

Prior to use, the data is subjected to multiple preparation procedures. After downloading the CRyPTIC_reuse_table_20240917.csv file from the official compendium website, we chose to focus on two drugs: Rifampicin (RIF), which is primarily used to treat tuberculosis by inhibiting RNA polymerase, and Rifabutin (RFB), a related rifamycin derivative with similar therapeutic applications.

First, we filter the dataset to include only high and medium quality samples, based on the {drug}_PHENOTYPE_QUALITY field. This results in **10,310 samples** for **RIF** and **11,392 samples** for **RFB**. For each selected sample, we download its corresponding VCF file, which contains variant information. Then we remove columns with missing data and retain only entries marked as PASS in the FILTER field, indicating reliable variant calls.

To reduce dimensionality and reliability, we focus on positions where the ALT allele differs from the REF allele, discarding entries such as 0/0 and 0|0, which indicate homozygous reference (no variant), as well as ./ and .|., which denote missing or uncalled genotypes, it should be noted that the slash (/) unphased genotype, while the pipe (|) indicates a phased genotype. Variants are represented as pos_ref>alt for all alleles separated by commas; we refer to this representation as the *Path-1 Input*, after this filtering, we end up with a total of **417,635 unique variants**.

We also retain additional descriptive features for each variant: ['GT', 'DP', 'DPF', 'COV', 'FRS', 'GT_CONF', 'GT_CONF_PERCENTILE']. Numeric features are scaled using min–max normalization, while categorical features are encoded. The FRS field, representing the fraction of reads supporting the genotype call (#reads supporting GT / total reads), ranges between 0 and 1; Higher FRS values indicate stronger confidence in the genotype, whereas missing or low values typically correspond to low coverage or filtered calls, and hence we chose to replace its missing values with zeros. For each sample, these features are organised into an array of shape (number of variants \times 8 features \times 1), referred to as the *Path-2 Input*, which will be used later in a 1D-CNN model. Arrays are padded as needed to ensure uniform length across samples.

It should be noted that the resulting samples are not aligned with each other. For example, sample one may have 20_A>G at index 0, while sample two has 13_C>T at the same index. This indicates that the variants are not ordered strictly by their genomic positions in the input vectors. Originally, the variants were sorted by position in the VCF file, but after filtering and preprocessing, some variants shifted in the vectors. This positional inconsistency across samples motivates the use of a *Permutation-Invariant Block (SAB)* in the model architecture.

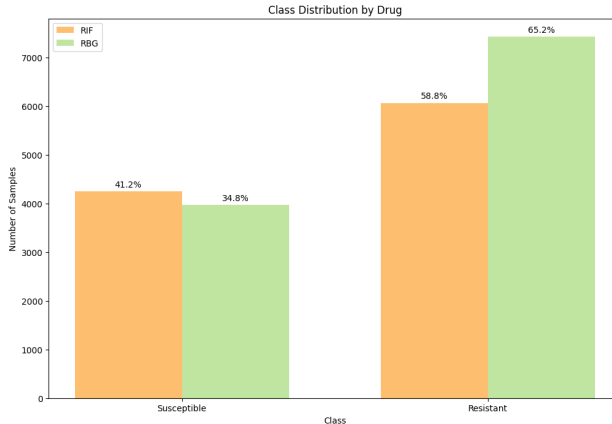


Figure 4: Distribution of classes for the selected drugs.

Figure 4 shows the class distribution of the two drugs, with a difference of $\sim 17.6\%$ between the susceptible and resistant class for *RIF*, and $\sim 30.4\%$ for *RFB*, requiring us to employ a weighted cross-entropy loss to handle this class imbalance.

We will first use the *RIF* data in all subsequent experiments, navigating several design choices to determine the optimal approach, and subsequently apply the selected method to *RFB* for validation.

5.2 Variants Encoding

As mentioned in Section 5.1, variants are represented as `Pos_REF>ALT`, with the `ALT` for each allele separated by a comma. We compare a *Static Encoding* method, where each variant is given a unique ID to represent it, against training a *BERT Tokenizer* on all unique variants, and then using it to encode each sample's variants into vectors before training.

The results showed that *Static Encoding* led to overfitting in the long run, with early stopping triggered at epoch 3. The training curve clearly showed signs of overfitting, with a $\sim 6.73\%$ gap between training and validation accuracy. In contrast, using *BERT* proved effective in delivering more stable learning and improved validation performance. Although it also showed signs of overfitting, with a 4.83% difference between training and validation accuracy at the end of training, it maintained a smoother learning curve and reached early stopping at epoch 16.

The *BERT*-based encoding was more robust and critical for stable learning as shown in Figure 5. Consequently, we selected *BERT* for the encoding phase in all subsequent experiments.

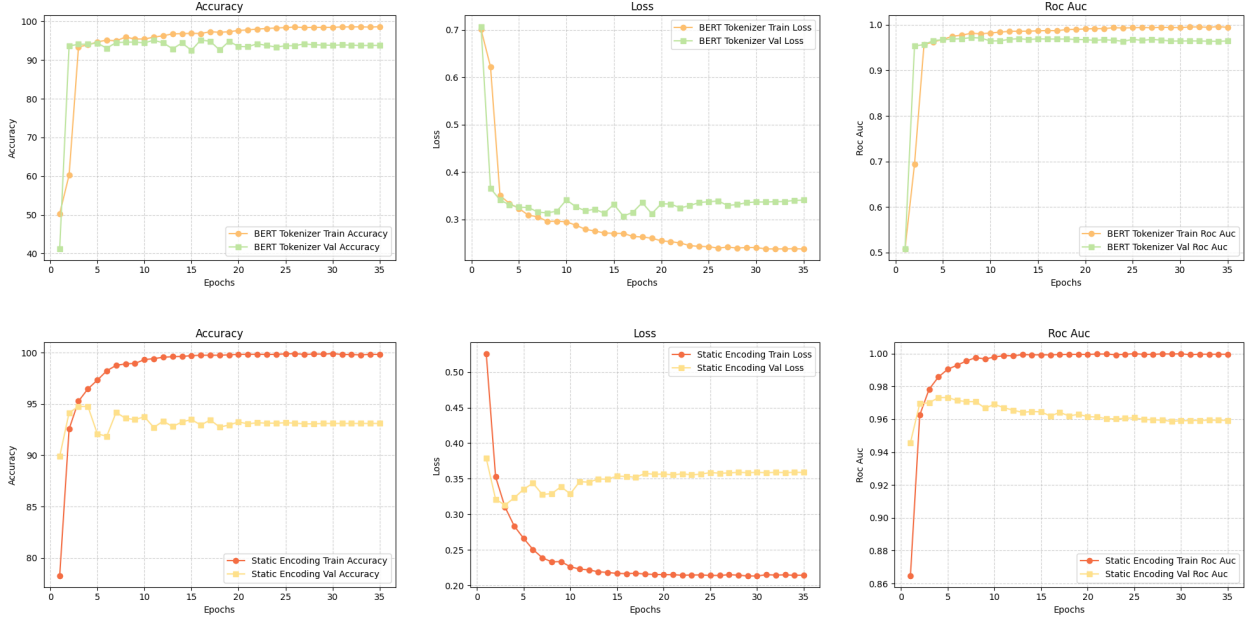


Figure 5: Comparison of Static Encoding vs BERT Tokeniser metrics over epochs

5.3 The Choice of Fusion Mechanism

We tested three types of fusion strategies between Path-1 and Path-2, namely: Suppression, Amplification, and Suppression-Amplification (see Section 4.2.3). The training and validation curves are shown in Figure 6 and the test results are summarized in Table 1.

All three types achieved comparable performance in terms of validation and test accuracy. However, in general, the *Amplification fusion* yielded the best results and, therefore, it was selected as the preferred mechanism for the final configuration, and we will refer to this model as - *Model A* -.

Table 1: Comparison of fusion mechanisms. Best results in bold

Fusion Type	Accuracy	Precision	Recall	F1	AUC
Suppression & Amplification	0.9267	0.9322	0.9439	0.9381	0.9572
Amplification	0.9523	0.9510	0.9598	0.9554	0.9690
Suppression	0.9438	0.9460	0.9591	0.9525	0.9710

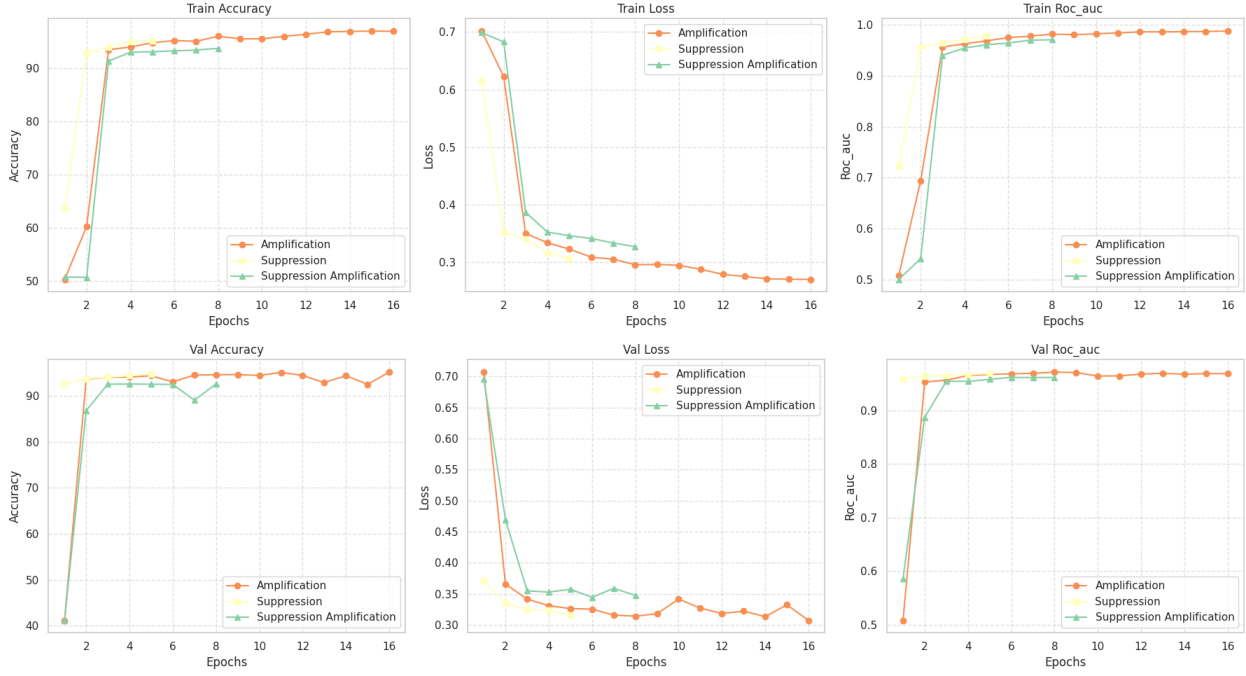


Figure 6: Training (top) and validation (bottom) performance curves for fusion methods

5.4 Models Experimentation

Starting from - *Model A* - , we evaluated a set of configurations to measure the robustness of the padding/masking strategy, data augmentation, and to assess the benefits of including Path-2 in the architecture. Moreover, we compared with a traditional approach, adopted in many studies, which involved representing the data as a matrix of shape *(Number of Variants) × (Number of Samples)*, where cell i, j is 1 if Variant- i is present in the sample, otherwise 0. This representation is typically trained with classifiers using either classical machine learning or deep learning techniques such as CNNs or MLP-based models. This hybrid of simple binary encoding and deep models has been widely surveyed in antimicrobial resistance (AMR) and clinical genomics literature and has been effective in practice (e.g., CNN and ML studies for tuberculosis and other pathogens) [Sakagianni et al., 2024]. However, one limitation of this approach is the large resulting sparse matrix due to the high number of variants, i.e., the curse of dimensionality, requiring extensive computational resources. Some studies addressed this by pre-eliminating variants using statistical methods, or dimensionality reduction techniques like PCA [Reshetnikov et al., 2025, Pikalyova et al., 2024, Xu et al., 2025].

To select informative variants, we applied a Chi-squared test to assess the association between each variant and the target phenotype. Variants with p -value < 0.001 were retained, resulting in 11,567 ($\sim 36.1\%$ reduction), which were then used to train and evaluate both a multi-layer perceptron (MLP) and a convolutional neural network (CNN).

To systematically evaluate the contributions of the proposed components, we developed and tested several distinct model architectures:

1. **Model-A:** SAB with Attention Masks for Padding, without Augmentation.
2. **Model-B:** SAB without Attention Masks for Padding, with Augmentation.

3. **Model-C**: SAB without Attention Masks for Padding, without Augmentation.
4. **Model-D**: SAB without Attention Masks for Padding, with Augmentation.
5. **Model-E**: Model-A settings, without the inclusion of Path-2.
6. **Model-F**: Model-B settings, without the inclusion of Path-2.
7. **Model-G**: MLP for Presence/absence Variants data.
8. **Model-H**: CNN for Presence/Absence Variants data.

Table 2: Best hyperparameters of -*Path-1* - for each proposed Multi-Path model applied on RIF Drug + *Model A* on RFB Drug

Model	Emb Dim	Hidden Dim	Num Layers
Model A	64	32	3
Model B	64	32	2
Model C	128	32	1
Model D	64	32	3
Model E	128	32	4
Model F	64	32	1
Model A (RFB)	128	32	1

Table 3: Best hyperparameters of - *Path-2* - and the Classification head for each proposed Multi-Path model applied on RIF Drug + *Model A* on RFB drug

Model	Dropout	Activation	Conv Layers	Conv Kernel	LR
Model A	0.1128	relu	3	3	0.00137
Model B	0.0962	gelu	2	5	0.00165
Model C	0.3817	gelu	1	5	0.00130
Model D	0.0205	gelu	3	3	0.00101
Model E	0.0692	relu	–	–	0.00105
Model F	0.3634	gelu	–	–	0.00154
Model A (RFB)	0.2704	relu	4	5	0.00106

Table 4: Best hyperparameters of MLP model aplied on RIF Drug

Model	Hidden Dims	Dropout	Activation
Model G	[1024, 128, 128]	0.1315	gelu

Table 5: Best hyperparameters of CNN model applied on RIF Drug

Model	Dropout	Activation	Conv Layers	Filters	Kernel Sizes	Pool Sizes
Model H	0.1487	relu	3	[96, 128, 256]	[5, 9, 2]	[3, 3, 3]

The proposed models were evaluated across multiple architectures and hyperparameter configurations. Tables 2, 3, 4, and 5 summarize the best-performing hyperparameters identified through Bayesian optimization. This tuning prioritized a balance between ROC AUC and Accuracy on the validation set, ensuring that models not only fit the training data but also generalized robustly.

In Figure 7, we compare the performance of *Model-A* and *Model-B* where *Model-B* applies data augmentation via variant sequence shuffling. This augmentation fully leverages the SAB block’s capacity, allowing predictions independent of variant position. Training curves confirm that *Model-B*, likely due to the regularization effect of data augmentation, exhibits greater training stability as evidenced by significantly reduced overfitting and closer convergence between the training and validation curves. On the test set, *Model-A* achieved the highest performance (ROC AUC: 0.969, Balanced Accuracy: 0.945). While *Model-B*’s test performance was marginally lower (ROC AUC: 0.964, Balanced Accuracy: 0.941), this minor trade-off in peak performance resulted in a substantially more robust and stable model. This suggests

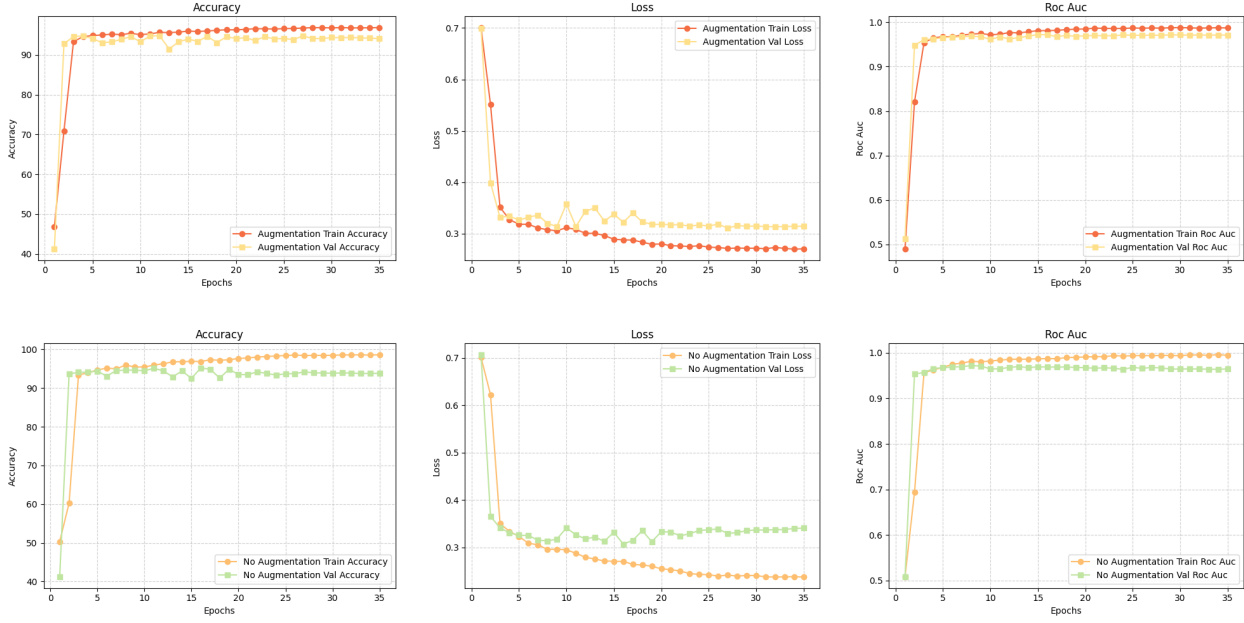


Figure 7: Comparison of -Model A- and -Model B- performance without and with variant sequence shuffling for training and validation

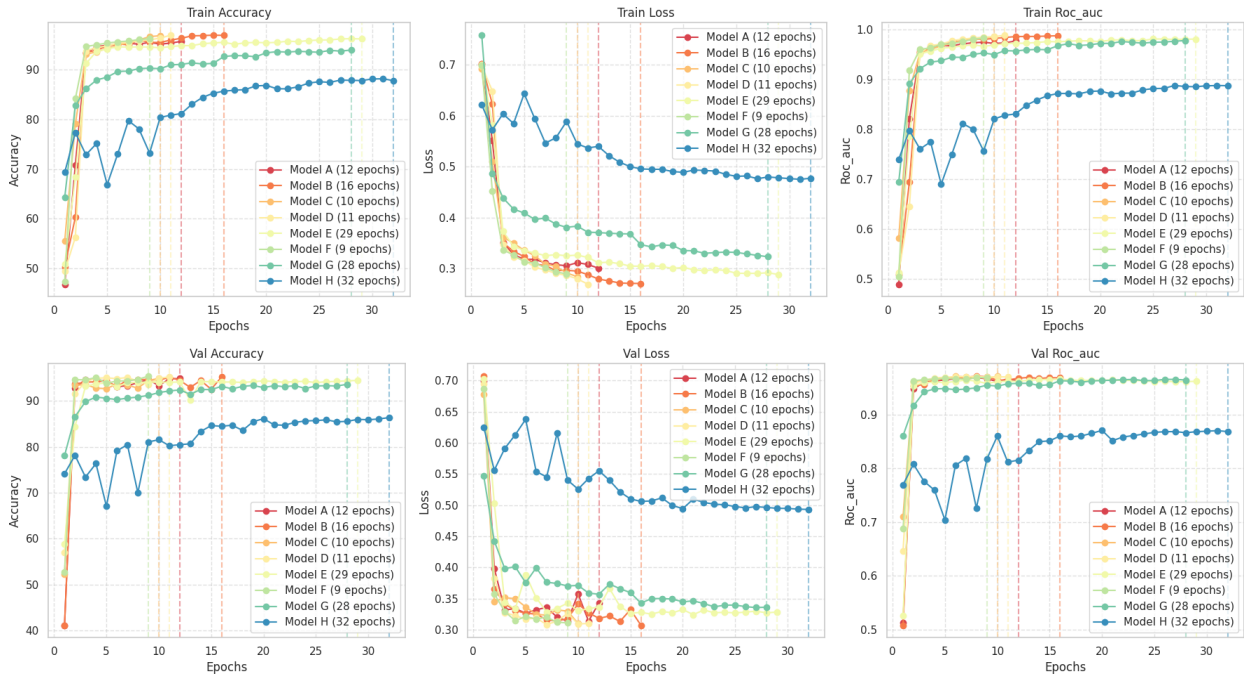


Figure 8: Training (top) and validation (bottom) performance curves of all models with early stopping

that data augmentation effectively improves generalization and stability with only a negligible decrease in maximum predictive power.

Figure 8 presents the training and validation curves across epochs for eight distinct models (Model-A through Model-H), offering critical insight into their convergence, learning capacity, and generalization ability.

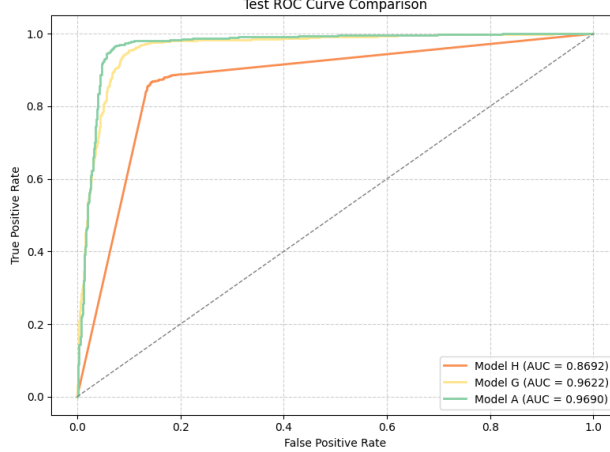


Figure 9: ROC AUC Test curve of VAMP-Net vs CNN and MLP

All models exhibit rapid initial learning, achieving 85% to over 90% accuracy within the first 5 to 10 epochs. The models can be broadly categorized into three performance tiers based on their final stabilized validation accuracy and AUC. Models A, B, C, and D demonstrate the highest potential, peaking around 94%. Models G and H show comparatively lower learning capacity for this task, suggesting architectural limitations and insufficient model capacity. Models G and H required the longest training durations, this is a characteristic of models with less efficiency.

Model-A achieved the highest overall training and validation accuracy and AUC within the shortest training time, making it the most efficient high-performer. This demonstrates that *Path-2* inclusion significantly improved robustness and that SAB-based transformers outperform classical CNN/MLP representations. The lower performance of Models G and H suggests that these architectures are less suitable for the current task, as shown in Figure 9.

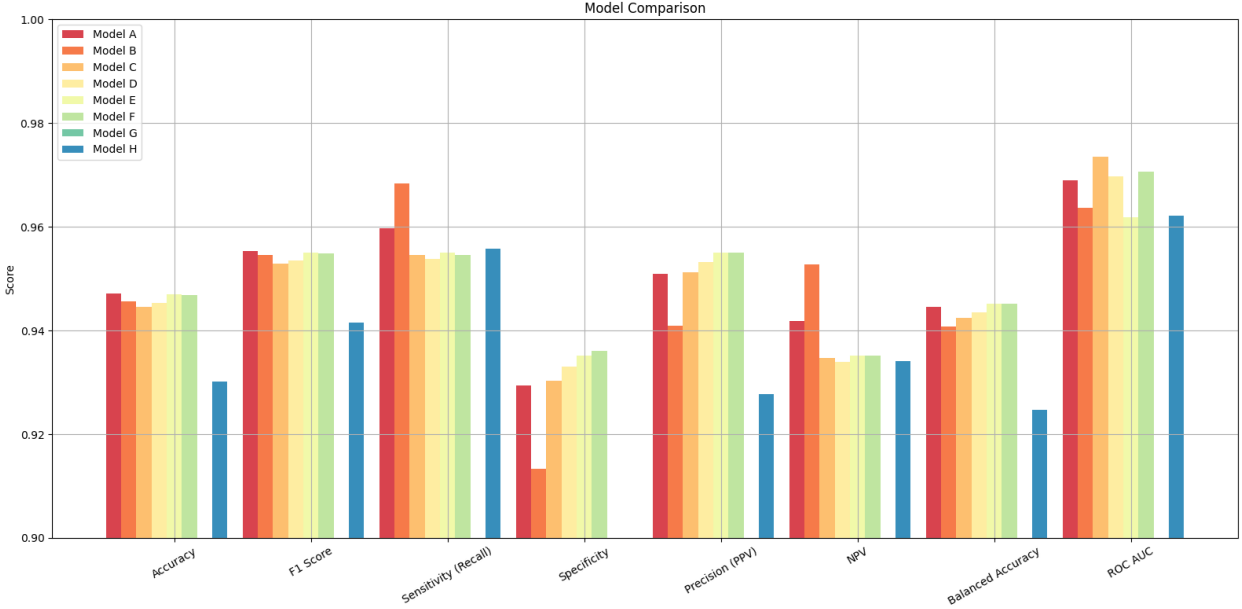


Figure 10: Models test results comparison

The results, visualized in Figure 10, clearly demonstrate the superior performance of the Set Attention Block (SAB)-based transformer architectures. While *Model-A* achieved the highest overall performance, the marginal variation across other SAB variants underscores the robustness of the core attention mechanism. Notably, the impact of explicit masking appears minimal, as evidenced by the comparable performance of Models C and D, suggesting that the SAB structure

inherently handles or ignores padding tokens effectively. In contrast, the significant underperformance of the traditional Multilayer Perceptron (MLP) (Model G) and Convolutional Neural Network (CNN) (Model H) strongly validates the utility of a sequential attention-based representation over standard binary encoding or fixed-filter approaches for this task.

Based on its performance across all evaluation metrics, we selected *Model-A* as the optimal architecture. To validate the model’s capacity for broad applicability, we applied this model on the *RFB* drug. On this drug, *Model-A* demonstrated high efficacy, achieving an AUC of 0.9681 and an Accuracy of 0.9393. Furthermore, the model maintained a well-balanced classification profile, yielding an F1 score of 0.9535, a Recall of 0.9553, and a Precision of 0.9517. These results collectively confirm the model’s excellent generalization capacity across different therapeutic agents.

The comprehensive architectural evaluation leads to the following four key conclusions:

- Superiority of Attention: Set Attention Block (SAB)-based transformer architectures significantly outperform standard Convolutional Neural Network (CNN) and Multilayer Perceptron (MLP) baselines on presence/absence data.
- Enhanced Generalization: Augmentation (as employed in *Model-B*) effectively improves training stability and promotes permutation invariance, leading to more robust models.
- Architectural Robustness: While empirically minor, the inclusion of attention masks provides critical robustness against padding tokens, formalizing the model’s ability to handle variable-length sequences.
- Broad Applicability: The high performance achieved on the *RFB* drug dataset validates the broad applicability and transferability of the SAB-based transformer approach to new, unseen drugs.

5.5 Multi-Path Framework Analysis and Interpretation

This section presents the results of the Dual-Path Interpretability Framework and leverages the insights to dissect the model’s decision-making process for *RIF* and *RFB* resistance prediction. Our analysis demonstrates that the two architectural pathways within *VAMP-Net* provide distinct yet complementary perspectives on the underlying mechanisms of drug resistance. Specifically, Path-1 (Set Attention Transformer) successfully identified and quantified variant-level importance and epistatic dependencies, thus elucidating the core genetic drivers. In contrast, Path-2 (Quality-Aware CNN) focused on quantifying the influence of technical confidence metrics, revealing how the model performs noise regularization and feature calibration. By integrating the findings from both streams, our framework provides a comprehensive and auditable explanation of the model’s decision process —both biological and technical—that drives the final drug resistance classification.

5.5.1 Set-Transformer Genetic Variant Importance

This section details the quantitative analysis of individual variant contributions to drug resistance, as determined by the Integrated Gradients (IG) method applied to the SAB pathway (Path-1). The IG-derived attribution scores, aggregated across the test cohort, establish an empirically derived ranking of mean importance for all unique *ChromPos_Ref>Alt* variants. This analysis serves to validate the model’s ability to prioritize known resistance drivers while simultaneously discovering highly-ranked non-canonical variants that warrant further investigation. The subsequent analyses distinguish between the variant importance profiles learned for Rifampicin (RIF) and Rifabutin (RFB), highlighting the model’s discriminatory power.

A) Drug 1: RIF Resistance Analysis The analysis of the *VAMP-Net* pathway for *RIF* resistance achieved strong validation success, presented in Table 6, demonstrating the framework’s ability to learn and prioritize fundamental genetic mechanisms as reported in the literature [Teleni et al., 1993, Ramaswamy and Musser, 1998]. The identified variants in *rpoB*, *katG*, and other genes align with established resistance mechanisms documented in the WHO catalogue of mutations associated with drug resistance [Organization, 2023].

The model assigned primary predictive importance to variants within the RNA polymerase β subunit (*rpoB*) gene. Multiple high-confidence variants in Table 6, including 761139_C>A, 761101_A>T, and 761140_A>T, are located within the *rpoB* gene and fall precisely within the Rifampicin Resistance-Determining Region (RRDR). This alignment with established clinical and molecular biology literature validates the framework’s capacity to learn fundamental resistance pathways [Musser, 1995].

Beyond the primary *rpoB* target, the *VAMP-Net* successfully extracted complex, multi-gene resistance signatures. The model assigned high importance scores to variants associated with isoniazid resistance, including mutations

Table 6: Among 200 Top-Ranked Variants from RIF Resistance Analysis out of 417,635 Unique Variants

Variant	Importance Score	Gene
761139_C>A	0.178	<i>rpoB</i>
761101_A>T	0.116	<i>rpoB</i>
761140_A>T	0.058	<i>rpoB</i>
761154_TCG>TTC	0.050	<i>rpoB</i>
761108_GGA>GTT	0.044	<i>rpoB</i>
760314_G>T	0.029	<i>rpoB</i>
2155162_ATGCCGC>ACGCCGT	0.446	<i>katG</i>
2155166_CGC>CTG	0.043	<i>katG</i>
7581_G>T	0.050	<i>gyrA</i>
4247574_A>C	0.036	<i>embB</i>
1849861_G>T	0.207	<i>ethA</i>
2338202_CAC>CCAC	0.308	<i>ponA1</i> (novel)
424791_T>TAT	0.273	<i>pknB</i> (novel)

in the *katG* region (2155162_ATGCCGC>ACGCCGT) and the promoter of *ahpC* (78519_G>A) [Vilchèze and Jacobs, 2007, Napier et al., 2023]. This demonstrates the framework's ability to capture complex multi-drug resistance profiles where resistance to one drug often co-occurs with markers for another [Jia et al., 2021, Billows et al., 2024].

A significant finding is the identification of top-ranked variants located in previously uncharacterized genomic regions (Novel loci). The high Importance Scores for these novel variants (such as *ponA1* and *pknB*) suggest the model is uniquely capable of isolating:

- **Rare, High-Effect Mutations:** Highly penetrant variants that evade detection by standard frequency-based GWAS methods.
- **Critical Interaction Hubs:** Loci that function as epistatic modifiers, significantly altering the expression or effect of primary resistance mutations.

In summary, the high attribution results confirm the robustness and superior discovery potential of the *VAMP-Net*, which can simultaneously validate known mechanisms and identify high-impact novel loci for targeted functional investigation.

B) Drug 2: RFB Resistance Analysis The *RFB* resistance analysis successfully identified the complete spectrum of variants associated with the phenotype (Table 7), confirming the model's high fidelity in identifying key resistance mechanisms.

Table 7: Among 200 Top-Ranked Variants from RFB Resistance Analysis out of 417,635 Unique Variants

Variant	Importance Score	Gene
761140_A>T	6.896	<i>rpoB</i>
761139_C>A	3.955	<i>rpoB</i>
761140_A>G	3.321	<i>rpoB</i>
761110_A>G	3.316	<i>rpoB</i>
761110_A>T	2.463	<i>rpoB</i>
4247431_G>T	2.125	<i>embB</i>
7581_G>A	1.323	<i>gyrA</i>
2944085_C>T	4.947	<i>mmpL5</i> (novel)
893702_GAC...CCG	4.213	<i>lpqS</i> (novel)
3640407_G>A	3.532	<i>ppsD</i> (novel)
3545402_A>G	3.527	<i>fadD26</i> region (novel)
1262023_C>T	2.885	<i>pks13</i> (novel)
4217696_TGGAG>TTGAA	2.594	<i>papA4</i> (novel)
1262193_C>T	2.589	<i>pks13</i> (novel)

The analysis demonstrated the framework's superior capability to identify both canonical and non-canonical resistance mechanisms. As expected, *rpoB* coding region variants ranked most highly, with the top-scoring variant 761140_A>T (Score 6.896) confirming the model's alignment with the shared target mechanism between RFB and RIF [Williams et al., 1998, Van Deun et al., 2013, Wang et al., 2023]. Multiple additional *rpoB* variants achieved high scores, including 761139_C>A (Score 3.955), 761140_A>G (Score 3.321), 761110_A>G (Score 3.316), and 761110_A>T (Score 2.463), all clustering within the Rifampicin Resistance-Determining Region (RRDR).

Furthermore, the framework successfully captured a Multi-Drug Resistance (MDR) genomic signature from a single drug prediction task. The detection of relevant variants in *embB* (4247431_G>T) and *gyrA* (7581_G>A) confirms the learned importance of co-selection and cross-resistance patterns [Ghosh et al., 2020].

The discovery potential of the framework is underscored by the high ranking of numerous novel variants. High scores for variants in genes such as *mmpL5* (2944085_C>T, Score 4.947), *lpqS* (893702_GAC...CCG, Score 4.213), *ppsD* (3640407_G>A, Score 3.532) reinforce the strong suggestion that these uncharacterized loci represent crucial epistatic interaction points or rare, high-effect genes that contribute significantly to the RFB phenotype. These variants are now prime candidates for functional validation to uncover new biological resistance pathways.

5.5.2 Genetic Variant Interaction Network Analysis

Analysis of the aggregated Set Attention Block (SAB) weights culminates in the Multi-locus Attribution-Weighted Interaction (MAWI) Map (Figures 11 and 12), which provides a critical, quantifiable decomposition of complex, multi-locus epistatic effects underlying Rifampicin (RIF) and Rifabutin (RFB) resistance. This approach moves beyond single-variant association models to capture the necessary synergistic coordination between mutations. Specifically, the heatmaps visualize the highest magnitude of attention-weights found by the SAB transformer, thereby mapping the strength and direction of these interactions and providing mechanistic insights into the polygenic architecture of drug resistance.

The variant interaction heatmap (Figure 11) for *RIF* (Rifampicin) resistance reveals a highly interconnected, yet structured, network of epistatic relationships among the top hub variants, with a high overall signal density indicating numerous strong-to-moderate synergistic interactions. This high-interaction density suggests that robust resistance relies on compensatory or cooperative pathways, confirming that the model has effectively learned the structural dependencies of a highly interconnected resistance mechanism. The pattern is characterized by specific "hub" variants, such as 3829770_T>C and 1307598_C>G, which act as central nodes, exhibiting dark red cells that indicate strong attention to multiple other variants in the network. This hub-driven structure supports the idea that the mechanism relies on a few key "linchpin" mutations that coordinate with a set of secondary, supportive mutations, and this strong cross-attention quantitatively supports the hypothesis of epistatic fitness compensation. Furthermore, the scattered distribution of high-value cells across the map, rather than being localized to a single cluster, suggests a diffuse polygenic mechanism where many different combinations of mutations contribute significantly to the resistance phenotype.

The second heatmap in Figure 12 (blue-to-red scale, max interaction ≈ 0.40) depicts a contrasting, sparse network of high-magnitude, localized epistatic effects for *RFB* resistance. In contrast to Figure 11, this visualization shows a predominantly low-interaction background (dark blue), highlighting a few critical, high-leverage interactions that dominate the attention landscape involving variants like 1070702_T>C. The high attention-weights (dark red) pattern suggests that these specific variant interactions act as a primary mechanism for resistance, where the effect of one variant is highly dependent on the presence of the other. The sparsity indicates that, while many variants are present, only a select few combinations are mechanistically determinative, allowing the *VAMP-Net* model to pinpoint the most non-additive synergistic effects.

The contrasting patterns between the two drugs demonstrate that resistance involves coordinated resistance modules whose composition varies depending on the specific drug, providing a key insight for designing combination therapies. The MAWI provides an interpretable, quantitative visualization of complex genetic epistasis, confirming known biological interactions while highlighting high-impact, potentially novel interaction hubs.

5.5.3 VCF Feature Channel Analysis: Quantifying the Influence of Variant Quality Metrics

We quantified the contribution of the eight VCF features via systematic ablation, validating the unique multi-channel design of the Quality-Aware 1D-CNN pathway (Figure 13). This analysis highlights the technical robustness required

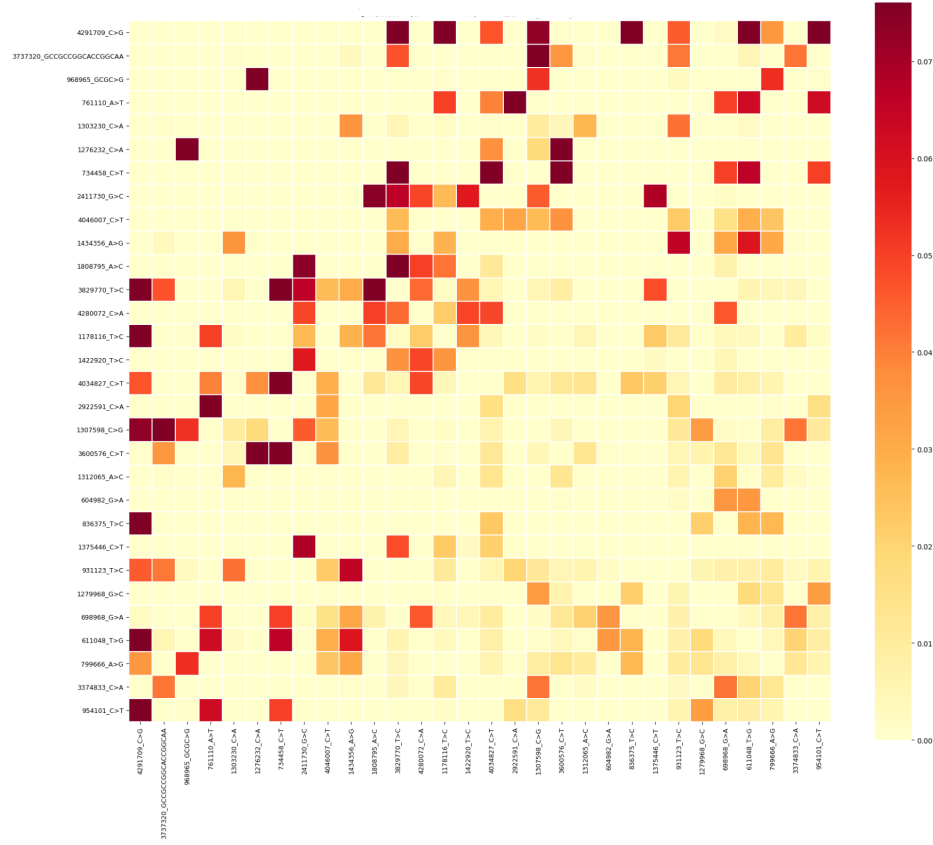


Figure 11: Variant interaction heatmaps showing attention-based relationships between top hub variants for RIF resistance. Red indicates strong interactions; yellow indicates weak interactions. The patterns reveal how variants work together in resistance mechanisms

for reliable genotype-phenotype association.

The analysis confirms the model does not rely on simple variant presence (GT field) but critically leverages the contextual quality and support metrics:

- Dominant Metric (*FRS*): The Fraction of Supporting Reads (*FRS*) is the single most influential feature for both the *RIF* and *RFB* models. This strong reliance confirms that the 1D-CNN pathway effectively learns to filter out false positives or low-support variants, as high *FRS* is used as a primary filter for calling true clonal mutations in MTB sequencing [Consortium, 2022].
- Contextual Confidence: The *GT_CONF_PERCENTILE* is the second most important feature. By utilizing the relative confidence rank rather than the raw *GT_CONF* (which shows minimal contribution), the model demonstrates its capacity to leverage comparative, sample-specific context for prediction.

The near-zero composite scores for features like *Read Depth (DP)*, *Genotype (GT)*, and Raw *GT_CONF* are equally informative. The low importance of *DP* suggests its information is effectively captured by the derived, normalized metrics (*FRS* and *GT_CONF_PERCENTILE*), rendering the raw depth redundant. This indicates that the presence of a variant or its raw confidence is insufficient; the model requires the granular, multi-dimensional context of the variant's support and relative quality to make high-confidence resistance predictions.

This ablation study confirms that the 1D-CNN pathway successfully extracts biologically and technically meaningful information from the VCF features, enabling a robust distinction between true resistance-conferring variants and lower-quality calls, especially critical for subtle phenotypes like *RFB* resistance.

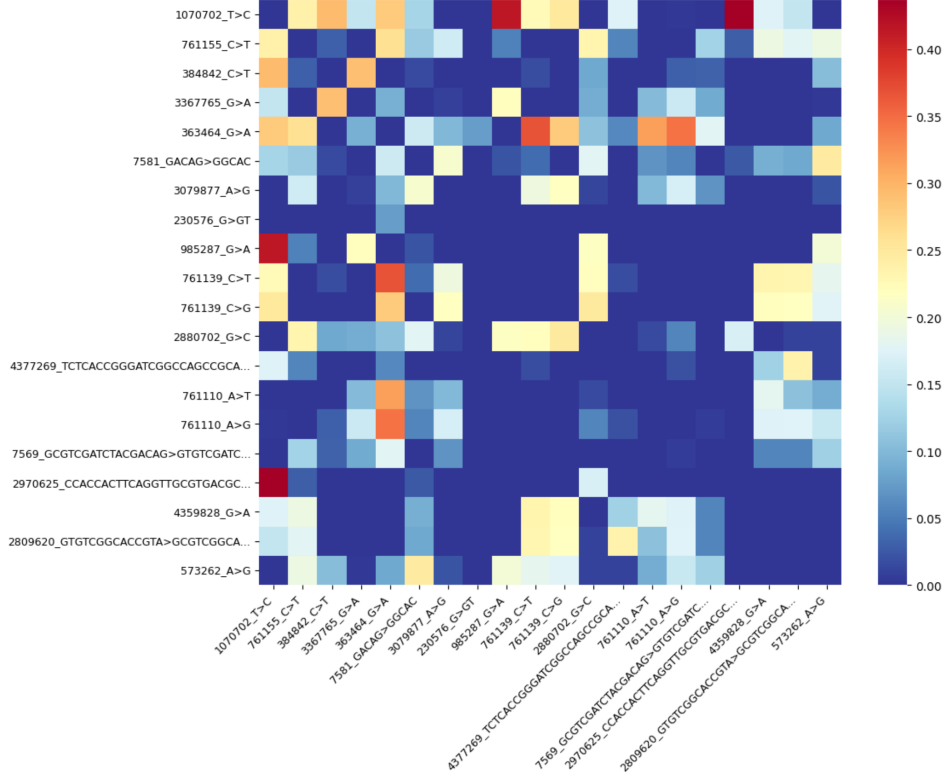


Figure 12: Variant interaction heatmaps showing attention-based relationships between top hub variants for RFB resistance. Red indicates strong interactions; blue indicates weak interactions. The patterns reveal how variants work together in resistance mechanisms

5.5.4 Dual-Path Fusion Model Interpretability

This final analysis validates the Multi-Path Fusion strategy as the core functional advancement of *VAMP-Net*, establishing its ability to combine Pathogenicity (via the Set-Transformer) and Reliability (via the 1D-CNN).

The analysis revealed two novel findings critical to the framework’s superior performance and generalizability:

- Learned Adaptive Feature Regularization: The 1D-CNN pathway functions as a learned signal-to-noise regulator, performing non-linear, context-aware feature selection (prioritizing *FRS* and *GT_CONF_PERCENTILE* over redundant features like *DP*). The most significant evidence of this is the 8 to 14-fold increase in feature reliance observed in the *RFB* model, which demonstrates that the fusion mechanism dynamically compensates for the weaker, more diverse genetic signal of that phenotype by demanding greater technical certainty. Path-2 thus acts as an adaptive attention mechanism that modulates prediction confidence based on data quality.
- Epistatic Network Auditing: The SAB network analysis confirmed that the final prediction is governed by an epistatic network audit, where the model learns that a high-importance variant from Path-1 will have its final impact dynamically down-weighted if Path-2 reports low sequencing support. This integrated approach provides an auditable, high-confidence score that addresses the critical challenge of separating biological signal from computational support in clinical genomic data.

In conclusion, integrating VCF features in this manner addresses a major challenge in genomic deep learning: the inherent separation between the biological signal (variant identity) and the computational support (variant quality).

6 Conclusion

We have introduced the Interpretable Variant-Aware Multi-Path Network (*VAMP-Net*), a novel deep learning framework that successfully addresses two critical, often-overlooked challenges in genomic machine learning: modeling genetic

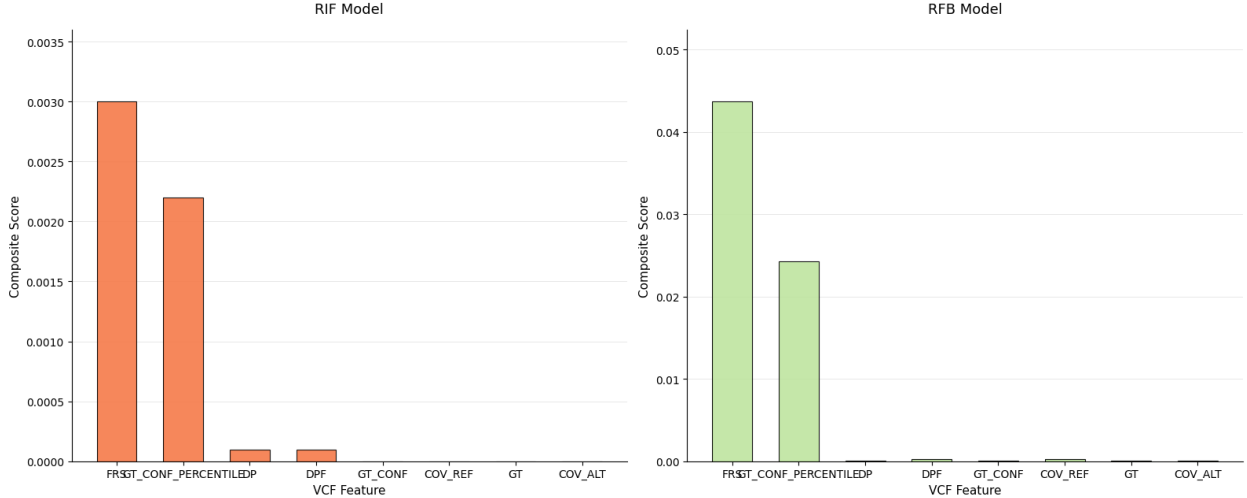


Figure 13: VCF feature importance comparison for RIF and RFB resistance models. Fraction of Supporting Reads (FRS) and Genotype Confidence Percentile (GT_CONF_PERCENTILE) demonstrate substantially higher importance for both resistance phenotypes, with the RFB model showing greater dependence on these quality metrics

epistasis and systematically incorporating variant calling quality into the prediction process. Our work delivers a significant methodological advance that provides both state-of-the-art predictive performance and crucial layers of auditable interpretability, essential for bridging computational genomics with clinical utility.

The core of *VAMP-Net* lies in its dual-path architecture and the Adaptive Fusion mechanism. The Set Attention Transformer (Path-1) proved highly effective by operating on the inherently permutation-invariant set of ChromPos_Ref>Alt variant tokens, successfully elucidating complex genetic epistasis and discovering both canonical resistance drivers and influential non-canonical loci. The Integrated Gradients attribution analysis provides a clear, ranked list of mutations and their co-dependencies, forming a direct basis for targeted functional validation.

However, the most compelling finding lies in the contribution of the Quality-Aware pathway. *VAMP-Net* is the first model to systematically integrate variant calling quality into resistance prediction, addressing the critical gap where existing methods treat all variant calls equally regardless of technical confidence. Our quantitative feature importance scores demonstrate that the fusion architecture performs a learned feature calibration and noise regularization. Specifically, the pronounced increase in reliance on VCF quality metrics (e.g., FRS, GT_CONF_PERCENTILE) for the more complex Rifabutin (RFB) phenotype, compared to Rifampicin (RIF), confirms the fusion mechanism intelligently and dynamically adapts its weighting based on the complexity and confidence requirements of the task. This dynamic weighting mechanism provides an unprecedented level of robustness.

The *VAMP-Net* framework's fundamental design is inherently generalizable and extends well beyond the context of Multi-drug resistance in *M. tuberculosis*. Our proposal can be applied to any genotype-phenotype problem characterized by three conditions:

- Variable-Length Inputs: The sample is defined by an unordered set of symbolic events (e.g., structural variants, somatic mutations in cancer, or transcriptomic changes).
- Epistatic Dependencies: The final phenotype is driven by complex interactions rather than single-gene effects.
- Heterogeneous Evidence: The symbolic input (genotype) is accompanied by quantitative, context-specific technical metadata (e.g., sequencing depth, coverage, or population frequency).

Future work will thus focus on extending this multi-path fusion paradigm to incorporate additional modalities in other clinical domains, such as incorporating image modalities (e.g., microscopy or histology) or longitudinal clinical metadata alongside genomic data. This work establishes a new standard for confidence and transparency in clinical AI systems by ensuring that all predictions are not only accurate but are driven by a mechanism that is transparent and auditable across both biological and technical evidence streams.

Data availability statements

The complete dataset used in this study is publicly available at [ftp.ebi.ac.uk/pub/databases/cryptic/release_june2022/](ftp://ftp.ebi.ac.uk/pub/databases/cryptic/release_june2022/).

References

Bingxing An, Xue Gao, Tianpeng Chang, Jiangwei Xia, Xiaoqiao Wang, Jian Miao, Lingyang Xu, Lupei Zhang, Yan Chen, Junya Li, et al. Genome-wide association studies using binned genotypes. *Heredity*, 124(2):288–298, 2020.

Janine Arloth, Gökcen Eraslan, Till FM Andlauer, Jade Martins, Stella Iurato, Brigitte Kühnel, Melanie Waldenberger, Josef Frank, Ralf Gold, Bernhard Hemmer, et al. Deepwas: Multivariate genotype-phenotype associations by directly integrating regulatory information using deep learning. *PLoS computational biology*, 16(2):e1007616, 2020.

Niloofar Arshadi, Billy Chang, and Rafal Kustra. Predictive modeling in case-control single-nucleotide polymorphism studies in the presence of population stratification: a case study using genetic analysis workshop 16 problem 1 dataset. In *BMC proceedings*, volume 3, page S60. Springer, 2009.

Nina Billows, Jody Phelan, Dong Xia, Yonghong Peng, Taane G Clark, and Yu-Mei Chang. Large-scale statistical analysis of mycobacterium tuberculosis genome sequences identifies compensatory mutations associated with multi-drug resistance. *Scientific reports*, 14(1):12312, 2024.

Aicha Boutorh and Ahmed Guessoum. Grammatical evolution association rule mining to detect gene-gene interaction. In *International Conference on Bioinformatics Models, Methods and Algorithms*, volume 2, pages 253–258. SCITEPRESS, 2014.

Aicha Boutorh and Ahmed Guessoum. Classification of snps for breast cancer diagnosis using neural-network-based association rules. In *2015 12th international symposium on programming and systems (ISPS)*, pages 1–9. IEEE, 2015.

Aicha Boutorh and Ahmed Guessoum. Complex diseases SNP selection and classification by hybrid association rule mining and artificial neural network—based evolutionary algorithms. *Engineering Applications of Artificial Intelligence*, 51:58–70, 2016.

Micaela E Consens, Ander Diaz-Navarro, Vivian Chu, Lincoln Stein, Housheng Hansen He, Alan Moses, and Bo Wang. Interpreting attention mechanisms in genomic transformer models: A framework for biological insights. *bioRxiv*, pages 2025–06, 2025.

CRyPTIC Consortium. A data compendium associating the genomes of 12,289 mycobacterium tuberculosis isolates with quantitative resistance phenotypes to 13 antibiotics. *PLoS biology*, 20(8):e3001721, 2022.

Erdal Cosgun and Min Oh. Exploring the consistency of the quality scores with machine learning for next-generation sequencing experiments. *BioMed Research International*, 2020(1):8531502, 2020.

Wouter Deelder, Sofia Christakoudi, Jody Phelan, Ernest Diez Benavente, Susana Campino, Ruth McNerney, Luigi Palla, and Taane G Clark. Machine learning predicts accurately mycobacterium tuberculosis drug resistance from whole genome sequencing data. *Frontiers in genetics*, 10:922, 2019.

Kazım Kivanç Eren, Esra Çınar, Hamza U Karakurt, and Arzucan Özgür. Improving the filtering of false positive single nucleotide variations by combining genomic features with quality metrics. *Bioinformatics*, 39(12):btad694, 2023.

Joverlyn Gaudillo, Jae Joseph Russell Rodriguez, Allen Nazareno, Lei Rigi Baltazar, Julianne Vilela, Rommel Bulalacao, Mario Domingo, and Jason Albia. Machine learning approach to single nucleotide polymorphism-based asthma prediction. *PloS one*, 14(12):e0225574, 2019.

Abhirupa Ghosh, Saran N, and Sudipto Saha. Survey of drug resistance associated gene mutations in mycobacterium tuberculosis, esophageal and other bacterial species. *Scientific reports*, 10(1):8957, 2020.

Anna G Green, Chang Ho Yoon, Michael L Chen, Yasha Ektefaie, Mack Fina, Luca Freschi, Matthias I Gröschel, Isaac Kohane, Andrew Beam, and Maha Farhat. A convolutional neural network highlights mutations relevant to antimicrobial resistance in mycobacterium tuberculosis. *Nature communications*, 13(1):3817, 2022.

Matthias I Gröschel, Martin Owens, Luca Freschi, Roger Vargas Jr, Maximilian G Marin, Jody Phelan, Zamin Iqbal, Avika Dixit, and Maha R Farhat. Gentb: A user-friendly genome-based predictor for tuberculosis resistance powered by machine learning. *Genome medicine*, 13(1):138, 2021.

Tamsin James, Ben Williamson, Peter Tino, and Nicole Wheeler. Whole-genome phenotype prediction with machine learning: Open problems in bacterial genomics. *Bioinformatics*, page btaf206, 2025.

Yanrong Ji, Zhihan Zhou, Han Liu, and Ramana V Davuluri. Dnabert: pre-trained bidirectional encoder representations from transformers model for dna-language in genome. *Bioinformatics*, 37(15):2112–2120, 2021.

Hongbing Jia, Yuhui Xu, and Zhaogang Sun. Analysis on drug-resistance-associated mutations among multidrug-resistant mycobacterium tuberculosis isolates in china. *Antibiotics*, 10(11):1367, 2021.

Sohee Kang, Sevtap Savas, Hilmi Ozcelik, and Laurent Briollais. Inferring gene network from candidate snp association studies using a bayesian graphical model: application to a breast cancer case-control study from ontario. *Human heredity*, 78(3-4):140–152, 2015.

Jee In Kim, Finlay Maguire, Kara K Tsang, Theodore Gouliouris, Sharon J Peacock, Tim A McAllister, Andrew G McArthur, and Robert G Beiko. Machine learning for antimicrobial resistance prediction: current practice, limitations, and clinical perspective. *Clinical microbiology reviews*, 35(3):e00179–21, 2022.

Xingyan Kuang, Fan Wang, Kyle M Hernandez, Zhenyu Zhang, and Robert L Grossman. Accurate and rapid prediction of tuberculosis drug resistance from genome sequence data using traditional machine learning algorithms and cnn. *Scientific reports*, 12(1):2427, 2022.

Oh-Seok Kwon, Myunghee Hong, Tae-Hoon Kim, Inseok Hwang, Jaemin Shim, Eue-Keun Choi, Hong Euy Lim, Hee Tae Yu, Jae-Sun Uhm, Boyoung Joung, et al. Genome-wide association study-based prediction of atrial fibrillation using artificial intelligence. *Open Heart*, 9(1), 2022.

Juho Lee, Yoonho Lee, Jungtaek Kim, Adam Kosiorek, Seungjin Choi, and Yee Whye Teh. Set transformer: A framework for attention-based permutation-invariant neural networks. In *International conference on machine learning*, pages 3744–3753. PMLR, 2019.

Qiao Liu, Fei Xia, Qijin Yin, and Rui Jiang. Chromatin accessibility prediction via a hybrid deep convolutional neural network. *Bioinformatics*, 34(5):732–738, 2018.

Yang Liu, Duolin Wang, Fei He, Juexin Wang, Trupti Joshi, and Dong Xu. Phenotype prediction and genome-wide association study using deep convolutional neural network of soybean. *Frontiers in genetics*, 10:1091, 2019.

Yanran Ma, Botao Fa, Xin Yuan, Yue Zhang, and Zhangsheng Yu. Sts-bn: An efficient bayesian network method for detecting causal snps. *Frontiers in Genetics*, 13:942464, 2022.

Malgorzata Maciukiewicz, Victoria S Marshe, Anne-Christin Hauschild, Jane A Foster, Susan Rotzinger, James L Kennedy, Sidney H Kennedy, Daniel J Müller, and Joseph Geraci. Gwas-based machine learning approach to predict duloxetine response in major depressive disorder. *Journal of psychiatric research*, 99:62–68, 2018.

Bettina Mieth, Alexandre Rozier, Juan Antonio Rodriguez, Marina MC Höhne, Nico Görnitz, and Klaus-Robert Müller. Deepcombi: explainable artificial intelligence for the analysis and discovery in genome-wide association studies. *NAR genomics and bioinformatics*, 3(3):lqab065, 2021.

Florian Mittag, Michael Römer, and Andreas Zell. Influence of feature encoding and choice of classifier on disease risk prediction in genome-wide association studies. *PloS one*, 10(8):e0135832, 2015.

James M Musser. Antimicrobial agent resistance in mycobacteria: molecular genetic insights. *Clinical microbiology reviews*, 8(4):496–514, 1995.

Gary Napier, Susana Campino, Jody E Phelan, and Taane G Clark. Large-scale genomic analysis of mycobacterium tuberculosis reveals extent of target and compensatory mutations linked to multi-drug resistant tuberculosis. *Scientific Reports*, 13(1):623, 2023.

Hannah L Nicholls, Christopher R John, David S Watson, Patricia B Munroe, Michael R Barnes, and Claudia P Cabrera. Reaching the end-game for gwas: machine learning approaches for the prioritization of complex disease loci. *Frontiers in genetics*, 11:350, 2020.

World Health Organization. *Catalogue of mutations in Mycobacterium tuberculosis complex and their association with drug resistance*. World Health Organization, 2023.

Guillermo Paredes-Gutierrez, Ricardo Perea-Jacobo, Héctor-Gabriel Acosta-Mesa, Efren Mezura-Montes, Jose Luis Morales Reyes, Roberto Zenteno-Cuevas, Miguel-Ángel Guerrero-Chevannier, Raquel Muñiz-Salazar, and Dora-Luz Flores. Predicting drug resistance in mycobacterium tuberculosis: A machine learning approach to genomic mutation analysis. *Diagnostics*, 15(3):279, 2025.

Vladislav Perelygin, Alexey Kamelin, Nikita Syzrantsev, Layal Shaheen, Anna Kim, Nikolay Plotnikov, Anna Ilinskaya, Valery Ilinsky, Alexander Rakitko, and Maria Poptsova. Deep learning captures the effect of epistasis in multifactorial diseases. *Frontiers in Medicine*, 11:1479717, 2025.

Karina Pikalyova, Alexey Orlov, Dragos Horvath, Gilles Marcou, and Alexandre Varnek. Predicting s. aureus antimicrobial resistance with interpretable genomic space maps. *Molecular Informatics*, 43(5):e202300263, 2024.

S Ramaswamy and James M Musser. Molecular genetic basis of antimicrobial agent resistance in mycobacterium tuberculosis: 1998 update. *Tubercle and Lung disease*, 79(1):3–29, 1998.

Kirill Reshetnikov, Daria Bykova, Konstantin Kuleshov, Konstantin Chukreev, Egor Guguchkin, Alexey Neverov, and Gennady Fedonin. Feature selection and aggregation for antibiotic resistance gwas in mycobacterium tuberculosis: a comparative study. *Frontiers in Microbiology*, 16:1586476, 2025.

Alberto Romagnoni, Simon Jégou, Kristel Van Steen, Gilles Wainrib, and Jean-Pierre Hugot. Comparative performances of machine learning methods for classifying crohn disease patients using genome-wide genotyping data. *Scientific reports*, 9(1):10351, 2019.

Aikaterini Sakagianni, Christina Koufopoulos, Petros Koufopoulos, Sofia Kalantzi, Nikolaos Theodorakis, Maria Nikolaou, Evgenia Paxinou, Dimitris Kalles, Vassilios S Verykios, Pavlos Myrianthefs, et al. Data-driven approaches in antimicrobial resistance: Machine learning solutions. *Antibiotics*, 13(11):1052, 2024.

Julian G Saliba, Wenshu Zheng, Qingbo Shu, Liqiang Li, Chi Wu, Yi Xie, Christopher J Lyon, Jiuxin Qu, Hairong Huang, Binwu Ying, et al. Enhanced diagnosis of multi-drug-resistant microbes using group association modeling and machine learning. *Nature Communications*, 16(1):2933, 2025.

Abhinav Sharma, Edson Machado, Karla Valeria Batista Lima, Philip Noel Suffys, and Emilyn Costa Conceição. Tuberculosis drug resistance profiling based on machine learning: A literature review. *The Brazilian Journal of Infectious Diseases*, 26(1):102332, 2022.

Rafaella E Sigala, Vasiliki Lagou, Aleksey Shmeliov, Sara Atito, Samaneh Kouchaki, Muhammad Awais, Inga Prokopenko, Adam Mahdi, and Ayse Demirkan. Machine learning to advance human genome-wide association studies. *Genes*, 15(1):34, 2023.

Princess P Silva, Joverlyn D Gaudillo, Julianne A Vilela, Ranzivelle Marianne L Roxas-Villanueva, Beatrice J Tiangco, Mario R Domingo, and Jason R Albia. A machine learning-based snp-set analysis approach for identifying disease-associated susceptibility loci. *Scientific Reports*, 12(1):15817, 2022.

Shanwen Sun, Benzhi Dong, and Quan Zou. Revisiting genome-wide association studies from statistical modelling to machine learning. *Briefings in Bioinformatics*, 22(4):bbaa263, 2021.

Amalio Telenti, Paul Imboden, Francine Marchesi, L Matter, K Schopfer, T Bodmer, D Lowrie, MJ Colston, and S Cole. Detection of rifampicin-resistance mutations in mycobacterium tuberculosis. *The Lancet*, 341(8846):647–651, 1993.

Armand Van Deun, Kya JM Aung, Valentin Bola, Rossin Lebeke, Mohamed Anwar Hossain, Willem Bram de Rijk, Leen Rigouts, Aysel Gumusboga, Gabriela Torrea, and Bouke C de Jong. Rifampin drug resistance tests for tuberculosis: challenging the gold standard. *Journal of clinical microbiology*, 51(8):2633–2640, 2013.

Arno van Hiltten, Steven A Kushner, Manfred Kayser, M Arfan Ikram, Hieab HH Adams, Caroline CW Klaver, Wiro J Niessen, and Gennady V Roshchupkin. Gennet framework: interpretable deep learning for predicting phenotypes from genetic data. *Communications biology*, 4(1):1094, 2021.

Catherine Vilchèze and William R Jacobs, Jr. The mechanism of isoniazid killing: clarity through the scope of genetics. *Annu. Rev. Microbiol.*, 61(1):35–50, 2007.

Haohan Wang, Tianwei Yue, Jingkang Yang, Wei Wu, and Eric P Xing. Deep mixed model for marginal epistasis detection and population stratification correction in genome-wide association studies. *BMC bioinformatics*, 20(Suppl 23):656, 2019.

Xinrui Wang, Donghong Yu, and Lu Chen. Antimicrobial resistance and mechanisms of epigenetic regulation. *Frontiers in cellular and infection microbiology*, 13:1199646, 2023.

Yu Wang, Zhonghua Jiang, Pengkuan Liang, Zhuochong Liu, Haoyang Cai, and Qun Sun. Tb-drop: deep learning-based drug resistance prediction of mycobacterium tuberculosis utilizing whole genome mutations. *BMC genomics*, 25(1):167, 2024.

DL Williams, L Spring, L Collins, LP Miller, LB Heifets, PRJ Gangadharam, and TP Gillis. Contribution of rpoB mutations to development of rifamycin cross-resistance in mycobacterium tuberculosis. *Antimicrobial agents and chemotherapy*, 42(7):1853–1857, 1998.

Cuiling Wu, Yiyi Zhang, Zhiwen Ying, Ling Li, Jun Wang, Hui Yu, Mengchen Zhang, Xianzhong Feng, Xinghua Wei, and Xiaogang Xu. A transformer-based genomic prediction method fused with knowledge-guided module. *Briefings in Bioinformatics*, 25(1), 2023.

Yi Xu, Ying Mao, Xiaoting Hua, Yan Jiang, Yi Zou, Zhichao Wang, Zubi Liu, Hongrui Zhang, Lingling Lu, and Yunsong Yu. Machine learning-based prediction of antimicrobial resistance and identification of amr-related snps in mycobacterium tuberculosis. *BMC Genomic Data*, 26(1):48, 2025.

Meng Yang, Lichao Huang, Haiping Huang, Hui Tang, Nan Zhang, Huanming Yang, Jihong Wu, and Feng Mu. Integrating convolution and self-attention improves language model of human genome for interpreting non-coding regions at base-resolution. *Nucleic acids research*, 50(14):e81–e81, 2022.

Zhuo Zhang, Yanwu Xu, Jiang Liu, and Chee Keong Kwoh. Identify predictive snp groups in genome wide association study: a sparse learning approach. *Procedia Computer Science*, 11:107–114, 2012.

Jian Zhou and Olga G Troyanskaya. Predicting effects of noncoding variants with deep learning–based sequence model. *Nature methods*, 12(10):931–934, 2015.

Jian Zhou, Chandra L Theesfeld, Kevin Yao, Kathleen M Chen, Aaron K Wong, and Olga G Troyanskaya. Deep learning sequence-based ab initio prediction of variant effects on expression and disease risk. *Nature genetics*, 50(8): 1171–1179, 2018.